sustainability

MDPI

Article

Policy-Driven Sustainable Saline Drainage Disposal and Forage Production in the Western San Joaquin Valley of California

Amninder Singh [1], Nigel W. T. Quinn [2,*], Sharon E. Benes [3] and Florence Cassel [3]

[1] Department of Environmental Sciences, University of California, Riverside, CA 92521, USA; asing075@ucr.edu
[2] HydroEcological Engineering Advanced Decision Support Group, Berkeley National Laboratory, Berkeley, CA 94720, USA
[3] Department of Plant Science, California State University, Fresno, CA 93740, USA; sbenes@csufresno.edu (S.E.B.); fcasselss@csufresno.edu (F.C.)
* Correspondence: nwquinn@lbl.gov; Tel.: +1-510-612-8802

Received: 29 April 2020; Accepted: 30 July 2020; Published: 7 August 2020

Abstract: Environmental policies to address water quality impairments in the San Joaquin River of California have focused on the reduction of salinity and selenium-contaminated subsurface agricultural drainage loads from westside sources. On 31 December 2019, all of the agricultural drainage from a 44,000 ha subarea on the western side of the San Joaquin River basin was curtailed. This policy requires the on-site disposal of all of the agricultural drainage water in perpetuity, except during flooding events, when emergency drainage to the River is sanctioned. The reuse of this saline agricultural drainage water to irrigate forage crops, such as 'Jose' tall wheatgrass and alfalfa, in a 2428 ha reuse facility provides an economic return on this pollutant disposal option. Irrigation with brackish water requires careful management to prevent salt accumulation in the crop root zone, which can impact forage yields. The objective of this study was to optimize the sustainability of this reuse facility by maximizing the evaporation potential while achieving cost recovery. This was achieved by assessing the spatial and temporal distribution of the root zone salinity in selected fields of 'Jose' tall wheatgrass and alfalfa in the drainage reuse facility, some of which have been irrigated with brackish subsurface drainage water for over fifteen years. Electromagnetic soil surveys using an EM-38 instrument were used to measure the spatial variability of the salinity in the soil profile. The tall wheatgrass fields were irrigated with higher salinity water (1.2–9.3 dS m^{-1}) compared to the fields of alfalfa (0.5–6.5 dS m^{-1}). Correspondingly, the soil salinity in the tall wheatgrass fields was higher (12.5 dS m^{-1}–19.3 dS m^{-1}) compared to the alfalfa fields (8.97 dS m^{-1}–14.4 dS m^{-1}) for the years 2016 and 2017. Better leaching of salts was observed in the fields with a subsurface drainage system installed (13–1 and 13–2). The depth-averaged root zone salinity data sets are being used for the calibration of the transient hydro-salinity computer model CSUID-ID (a one-dimensional version of the Colorado State University Irrigation Drainage Model). This user-friendly decision support tool currently provides a useful framework for the data collection needed to make credible, field-scale salinity budgets. In time, it will provide guidance for appropriate leaching requirements and potential blending decisions for sustainable forage production. This paper shows the tie between environmental drainage policy and the role of local governance in the development of sustainable irrigation practices, and how well-directed collaborative field research can guide future resource management.

Keywords: saline irrigation; drainage water reuse; EM-38; leaching requirement; forage; decision support

1. Introduction

This Special Issue of Sustainability focuses on environmental policy and governance issues related to sustainable salinity management. In this paper, we strive to show how a unique selenium contamination problem impacting irrigated agriculture resulted in State and federal environmental policy that fundamentally changed irrigation management in the San Joaquin Valley of California. We describe the agricultural stakeholder response to the new policy, and the development of a dedicated reuse facility that has provided irrigators time to develop sustainable management practices while maintaining local governance. We describe a research project geared to improve and optimize these practices, which involves the use of electromagnetic instrument technology and associated techniques to map the salinity on selected forage fields, and show how data provided by these techniques can be interpreted and used to further develop and calibrate a vadose zone simulation model for future decision support. We conclude with our future goal of bridging the gap between complex sensing techniques that result from the deployment of the EM38 instrument and sensor-informed transient model application, and the irrigator who relies primarily on his/her experience to gain knowledge. Our aim was to show the connectivity between environmental protection and irrigation sustainability policy, and irrigation practice and how research can provide decision support and lead to better resource management outcomes.

1.1. Background

Worldwide, it is estimated that 20% of the total farmlands and 33% of the irrigated lands are affected by soil salinity, and that by 2050, half of the farmlands will be salinized [1]. The western San Joaquin Valley (SJV) in the central part of California, USA, is a highly productive agricultural area affected by shallow water tables and soil salinity, as well as high concentrations of selenium and boron in subsurface tile drainage. Soil salinity arises in part due to the marine nature of the native soils and the importation of irrigation water from the Bay-Delta estuary, which contains salts [2,3]. A recent salinity assessment of the western SJV based on remote sensing data and analysis indicated that 0.32 million hectares of lands are salt-affected (i.e., soil electrical conductivity, $EC_e > 4$ dS m^{-1}) which represents 45% of the region [3,4]. The high agricultural productivity of the western SJV mostly stems from its practice of irrigation, and from the State's extensive network of canals, which convey irrigation water to its place of use. The SJV also relies on the winter snowpack of the eastern Sierra Nevada mountains, and a network of state, federal and locally owned reservoirs, to help overcome the impact of droughts and the regulation-induced water shortages that can reduce agricultural water supplies. The prospect of future climate change impacts, coupled with an increasing population, has created incentives for local water districts to look beyond traditional sources of water and consider supplies previously deemed too marginal or saline for their use as irrigation water.

The reuse of saline–sodic drainage water to irrigate salt-tolerant forage crops is an attractive and cost-effective alternative because it reduces the volume of water requiring disposal [5–7]. Saline–sodic waters are characterized by high salt contents (electrical conductivity ECiw > 4.0 dS m^{-1}) and high sodicity, i.e., an elevated sodium (Na^+) concentration relative to concentrations of calcium (Ca^{2+}) and magnesium (Mg^{2+}), as expressed by a sodium adsorption ratio (SAR) > 12. Various forages have been studied for their potential to be grown under Saline–sodic irrigation waters [8]. Suyama and others also examined the suitability of 'Jose' tall wheatgrass (*Thinopyrum ponticum*, formerly *Agropyron elongatum*, var. 'Jose'), creeping (syn. Beardless) wildrye (*Leymus* (syn. *Elymus*) *triticoides* var. 'Rio'), paspalum (*Paspalum vaginatum*, var. SeaIsle 1), bermudagrass (*Cynodon dactylum* var. 'Giant') and alfalfa (*Medicago sativa*, 50:50 mix of vars. 'Salado and 801S') under irrigation with saline drainage water. They concluded that 'Jose' tall wheatgrass and salt tolerant alfalfa varieties are the best options for high forage quality (measured as metabolized energy (ME)) and acceptable dry matter production.

Alfalfa is more sensitive to salinity than 'Jose' tall wheatgrass, but it produces higher yields and forage quality, and it is more profitable. Elevated yields were reported for improved varieties of alfalfa in a field study by [7] at soil salinities as high as 7 dS m^{-1} EC_e, and more recently, ref. [9] evaluated

different cultivars of alfalfa in a sand tank study and suggested that irrigation waters resulting in soil salinities of up to 6 dS m^{-1} EC_e could be used throughout the production cycle without any significant yield loss. In a three-year field trial, ref. [10] reported an average yield loss of only 11% for 21 improved varieties of alfalfa irrigated with very high EC waters (8–10 dS m^{-1}), which resulted in soil salinities of 10–15 dS m^{-1} EC_e for 0–150 cm soil depth in the last two years. Ref. [11] also found that alfalfa had much higher salt tolerance than previously established, based on the performance of three salt tolerant varieties grown in large pots and irrigated with saline water for 18 months. Likewise, the field study by [7] indicated that 'Jose' tall wheatgrass had a very high level of salinity tolerance, as after five years of saline drainage water application and soil salinities reaching 18 dS m^{-1} ECe, the forage was still producing 6–7 metric t ha^{-1}, albeit with a lower dry matter yield.

However, irrigation with saline waters, particularly those high in sodium, can negatively impact soil's physical and chemical properties, and crop yields. Careful management is therefore needed to minimize salt accumulation in the root zone and sustain forage production [2,5,12,13]. Drainage or well waters that are saline–sodic are more problematic due to the negative effect of sodium on soil structure and consequent reductions in water infiltration [14]. Being a conservative constituent, salts tend to accumulate in the crop root zone over time if the water supply is insufficient to provide adequate leaching, or if the drainage disposal is inadequate to provide the long-term removal of salts from the crop root zone. Ref. [12] developed a regional groundwater and hydro-salinity model to conduct long-term (57 year) simulations of soil salinity in western Fresno county in the SJV to replicate historic changes in soil salinity. The model showed that, although long-term irrigation helped to reduce root zone salinity across the study area throughout the second half of the 20th century, there were concerns for the continued leaching of dissolved salts and the salinization of deeper groundwater which could compromise the sustainability of irrigation practices that conjunctively use groundwater [12].

Vadose zone simulation models can help to minimize the salinity hazard in agricultural systems and reduce the environmental impact of salinity. Initial guidelines for managing saline irrigation waters were based on steady state analysis which assumed that (a) irrigation water infiltrated at a constant rate, irrespective of the irrigation frequency, (b) evapotranspiration stayed constant over the growing season and (c) that the salt concentration of the soil solution was constant at all times [15]. These steady-state models provide conservative estimates that over-predict the negative consequences of saline water irrigation and suggest higher leaching requirements than would be recommended using transient-state models [15–17]. Hence, a transient modeling approach was chosen for this study. However, this approach requires sufficient data to both calibrate and verify the model, but also serves as a useful framework for experimental design and the design of sensor networks to provide a complete set of essential model input data. Although the CSUID model selected for this study is not elaborated in this paper, it will serve as an essential tool for achieving the goal of SJRIP (San Joaquin River Improvement Project) system sustainability through the optimization of existing and future practices. One of the first steps towards estimating leaching requirements is to know the current state of salinity in the field. Soil salinity is a dynamic soil property that varies spatially, as well as temporally. It is important to determine the spatial distribution of salts in the field in all three dimensions (across the field and downward in the profile). Information on the salt distribution in the soil profile can be used to determine if irrigation volumes are appropriate, or to infer the net movement of salts in different parts of a field, which can be helpful in assessing the functionality of a subsurface drainage system (if it is installed).

1.2. Environmental Policy to Control Salt and Selenium Pollutant Loading

The selenium ecotoxicity disaster at Kesterson Reservoir in 1985 that caused reproductive failure in overwintering waterfowl became a landmark in time, signifying a change in attitude on the topic of agricultural return flows in California and throughout the USA (Quinn, 2020; [18–20]). Up until that time, the only major constituent of concern in agricultural return flows had been nitrate, because of its health impacts on newborn children and potential for water body eutrophication and salinity for its

slow erosion of crop yields when the applied water salinity exceeded a certain salinity threshold. What followed was a comprehensive research effort led by the University of California and research divisions within State and Federal resource agencies, and the rapid closure of the Kesterson Reservoir and the San Luis Drain—the conveyance that supplied the drainage storage ponds with subsurface agricultural drainage water from a 2360 ha tile drained area within the Westlands Water District [18]. This research tapped past and ongoing research in Australia, Egypt and Israel, and brought in collaborating scientists from these countries and around the world in search of solutions to this unique environmental crisis impacting California's agriculture. The State Water Resources Control Board (SWRCB), the regulatory agency responsible for water resource and water quality policy in the State of California, embarked on a comprehensive model development effort to guide control actions to minimize environmental contamination due to selenium, boron and salt loading from agriculture. The international literature on river basin water quality modeling yielded little in the way of software that could be directly applied to the San Joaquin River Basin (SJRB). Since the San Joaquin River was the main conduit for the export of these contaminants to the Sacramento–San Joaquin Delta and the San Francisco Bay, the SWRCB focused its effort on the San Joaquin River as a driver of environmental policy [21].

The San Joaquin River Input–Output model (SJRIO) [22] was the first attempt at developing water and contaminant mass balances in the Basin, and served as the conceptual basis for the San Joaquin Valley Drainage Program's final policy report, which attempted to provide a balanced and equitable fifty year plan that provided for irrigation sustainability while protecting the fish and wildlife resources of the Basin and minimizing socioeconomic impacts [18,20]. Any significant loss of agriculture in the western San Joaquin Valley was predicted to have significant negative community impacts on the disadvantaged communities on the westside of the SJV. This major five-year research and policy planning process was followed by the Grassland Bypass Project [23] in 1996, a negotiated pact between agricultural and environmental interests, which was extended from 1996 to 2019, which provided a period of adjustment for agricultural entities to achieve zero selenium load discharge in the drainage return flows to the San Joaquin River [23]. This pact was followed by the U.S. Environmental Protection Agency (EPA) mandated salinity and boron Total Maximum Daily Load (TMDL) for the lower San Joaquin River Basin [21], a policy-directed action mandated under US federal law to address polluted and impaired public water bodies. The U.S. TMDL approach has been a particularly effective policy-driven tool for pollution abatement, although it has primarily been applied to pollutants and sectors other than salinity and agriculture.

1.3. Grassland Bypass Project

The Grassland Bypass Project [23] was conceived as a potential recipe for long-term irrigated agriculture sustainability in the Grasslands subarea of the San Joaquin River Basin in response to the policy-driven moratorium on selenium contaminated tile drainage export from the Westlands Water District which threatened to curtail agricultural production. The 44,000 hectare Grasslands subarea (Figure 1) had a long history of drainage export to the San Joaquin River through approximately 160 km of earthen channels that ran through an area dedicated to seasonal waterfowl habitat—private duck clubs and State and Federal wildlife refuges. The approximately 160 private duck clubs and beef cattle operations had made use of the agricultural drainage return flows, especially in the seasonal wetland areas to the south of the city of Los Banos, oblivious to the potential hazards associated with selenium teratogenicity and bioaccumulation in invertebrates and other biota. While a replacement water supply was being negotiated with the US Bureau of Reclamation for the approximately 64,000 ha of combined seasonally managed wetlands within the Grasslands Ecological Area, agricultural entities looked at short-term solutions for the immediate plumbing problem for sustained drainage relief, and longer term solutions for sustainable irrigated agricultural production on some of the most fertile and productive agricultural soils in the San Joaquin Valley. After 6 years of negotiation that lasted from October 1990 until September 1996, the Grassland Bypass Project was finalized, allowing the agricultural entities temporary use of the northern 45 km portion of the federally-owned San Luis

Drain in order to remove this selenium- contaminated drainage (water with greater than 2 ppb Se) from the wetland channels. The Use Agreement signed with the US Bureau of Reclamation [23] recognized the policy goal of the long-term reduction of selenium export to the San Joaquin River by mandating the eventual elimination of all selenium export to the San Joaquin River, except as a result of major precipitation events causing uncontrollable flooding. In response, the agricultural draining entities established a reuse facility on several hundred hectares of low value, salt impacted agricultural land that has expanded over the past two decades to its current footprint of 2428 hectares. There was confidence that, during the term of the Use Agreement, affordable selenium treatment technologies would be developed that would allow environmentally safe selenium export to the San Joaquin River that met selenium concentration objectives (5 ppb) in the San Joaquin River and its west-side drainage tributaries [18].

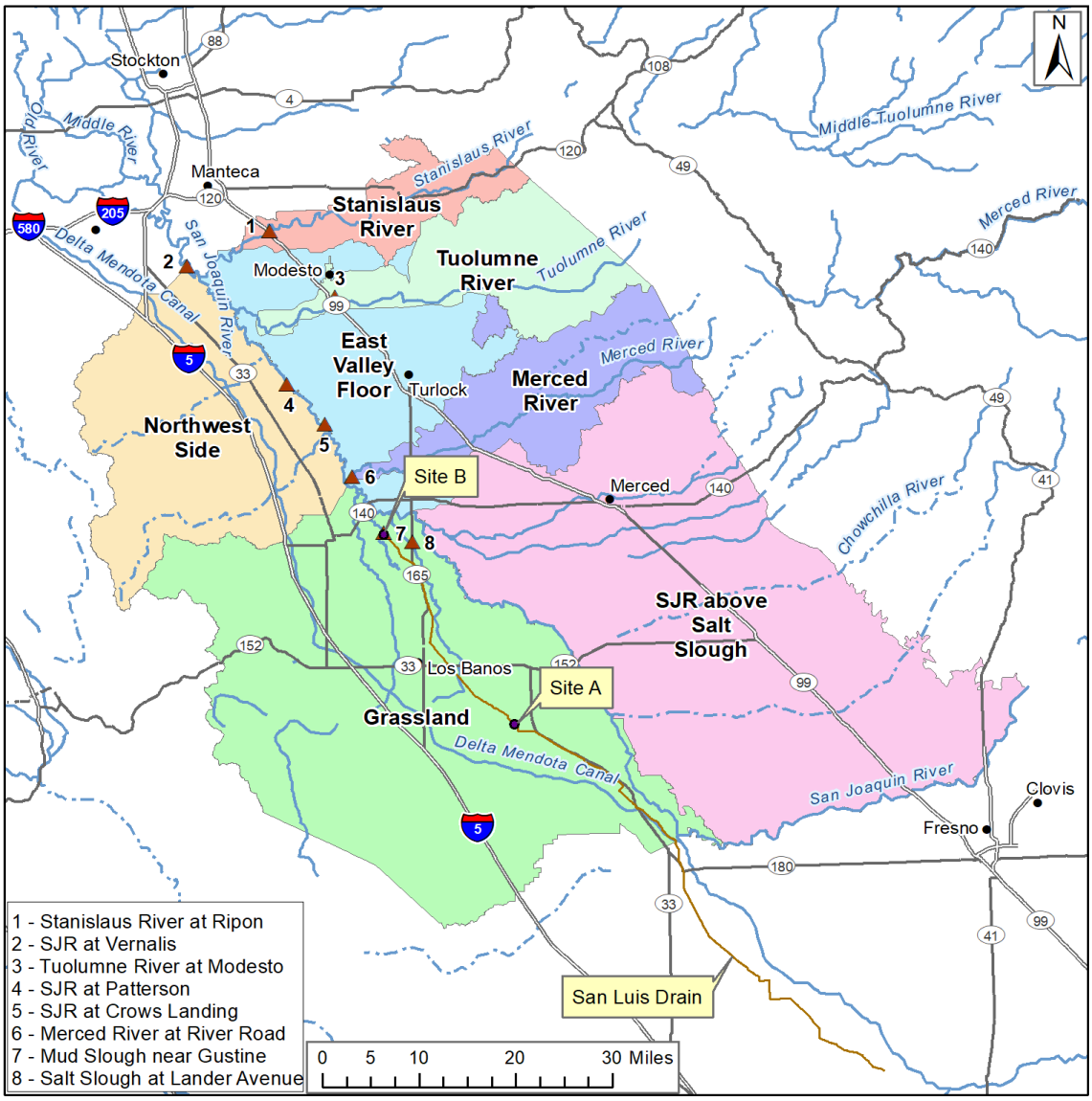

Figure 1. San Joaquin River Basin showing the Grasslands subarea, the Delta Mendota Canal that supplies irrigation water pumped from the Sacramento–San Joaquin Delta, and the San Luis Drain, which, until 31 December 2019, provided drainage relief to a 44,000 ha of highly fertile but selenium-contaminated agricultural land (U.S. Bureau of Reclamation, 2020).

In the USA in general, and California in particular, stakeholder and agency-initiated actions in response to major environmental policy mandates can take an inordinate amount of time, given the complex and sometimes contradictory mandates of the existing environmental laws and regulations, and the desire for consensus. The process for setting appropriate water quality objectives, even for constituents as simple as salinity, requires hearings to sort through the relevant underlying science and potential impacts for a myriad of stakeholder entities, and often lasts 5 to 10 years [21]. Although the Grassland Bypass project took six years of negotiation to gain final approval, it is regarded as one of the most successful policy-driven consensus environmental planning projects in the Basin's history.

1.4. San Joaquin River Improvement Project (SJRIP)

The drainage reuse facility was appropriately named the San Joaquin River Improvement Project (SJRIP) and has been the recipient of significant State and federal grants over the past twenty years, which have allowed the acquisition of contiguous land from willing sellers. An internal policy agreement was struck with the agricultural water districts that only subsurface agricultural drainage could be exported to the facility, which helped to minimize the volume of drainage requiring disposal. The subsurface drainage exported from each water district was combined in a central drain and exported to the SJRIP facility [3,15]. All of the surface drainage return flows and operational tailwater spill were collected in tailwater sumps where this water could be locally recycled on the same field or on-farm without co-mingling with subsurface drainage water. An innovative float, colored blue, yellow and red from top to bottom, was devised for deployment in field drainage sumps. These risers protruded from the ground and were visible from the road and to local by-passers. A sump riser showing red would indicate high water tables in a field—and likely poor water conservation practices—whereas a blue coloration would indicate relatively low water tables and less deep percolation. This and other internal policy directives allowed the close to real-time control of selenium drainage export, and close to 100% compliance with both the monthly and annual selenium load export limits that were mandated by the oversight committee for the Grasslands Bypass Project.

The Grassland Bypass Project [23] has been successful in meeting the program objectives and all selenium load targets except during the first two years of the project, in 1997 and 1998, when two back-to-back El Nino years resulting in exceedances of the nine-year mean monthly selenium loads that were established for the first three years of the Project. By 2012, the project had reduced the drainage discharge to the river by 82%, and salt, boron and selenium loads by 84%, 72% and 92%, respectively, as compared to the discharge in 1995 [16]. Monitoring was largely focused on selenium loading at the Site B compliance monitoring site (Figure 1), and at Site A immediately downstream, where the selenium drainage entered the San Luis Drain. In addition, discrete and continuous monitoring of water quality, sediments and biota was conducted in the Grasslands watershed. This was ostensibly to monitor any secondary impacts of the Project, and to ensure that agricultural Se-contaminated drainage remained excluded from wetland water supply delivery channels. Funding limitations and the general confidence in an eventual low-cost technological solution for selenium bioremediation and treatment did not extend the monitoring program to the SJRIP.

In recent years, evidence of declining crop yields in several alfalfa fields in the SJRIP have led to cropping changes, in which the more profitable alfalfa has been replaced with the less profitable, but more salt tolerant 'Jose' tall wheatgrass. Our study, described below, is the first comprehensive analysis in the SJRIP that attempts to address salt mass balance on alfalfa and 'Jose' tall wheatgrass fields, as well as drainage reuse sustainability issues in the San Joaquin River Basin. The objectives were to: (a) collect essential irrigation water and soil data in selected forage fields in the SJRIP, (b) to assess the spatial variability of salinity in the soil profile, and (c) to assess the sustainability of this forage production system for saline drainage disposal. The study also introduced the application of a simplified one-dimensional salinity simulation model, based on the Colorado State University Irrigation and Drainage Model (CSUID-1D), primarily as an initial framework to inform data collection. This model can eventually be used to guide water supply blending, leaching requirements and drainage

investment decisions. This decision support tool with a simple graphical user interface was designed for flexibility, in order to allow SJRIP facility personnel to fine-tune management practices for sustained forage yields using saline irrigation while achieving the prime purpose of the facility, which is drainage volume reduction and disposal.

2. Materials and Methods

2.1. Study Sites

The SJRIP (San Joaquin River Improvement Project) facility is located in western Fresno County, near the city of Firebaugh, California (USA) (Figure 1). It is bounded by the Delta Mendota Canal and the Central California Irrigation District's Main Canal to the south and north, respectively (Figure 1). The 2428-hectare facility is operated by the Panoche Water District (PWD) and provides drainage service to the Grasslands Drainage Area (GDA), located south of the city of Los Banos, between the San Joaquin River and Interstate 5. Less than 30% of fields within the GDA (i.e., 688 hectares) are installed with tile drains to help protect crops from water logging, and soils from accumulating salt through upward capillary flow. Over the past 20 years, several salt tolerant crops have been cultivated within the SJRIP and irrigated with subsurface drainage, and, in the case of several alfalfa fields, have been blended with pumped groundwater. The most successful crops have been 'Jose' tall wheatgrass, hereafter referred to as tall wheatgrass (TWG), and alfalfa hay (ALF), which now dominate the facility, with 1518 hectares and 384 hectares, respectively Most of the salt-tolerant crops are located on 1657 hectares, referred to as the SJRIP 1 (Figure 2). An additional 753 hectares, acquired in 2008, were planted with 1478 acres of salt-tolerant crops—referred to as SJRIP 2 in Figure 2. However, we will not be using this terminology henceforth, but rather 'SJRIP', referring to the entire facility.

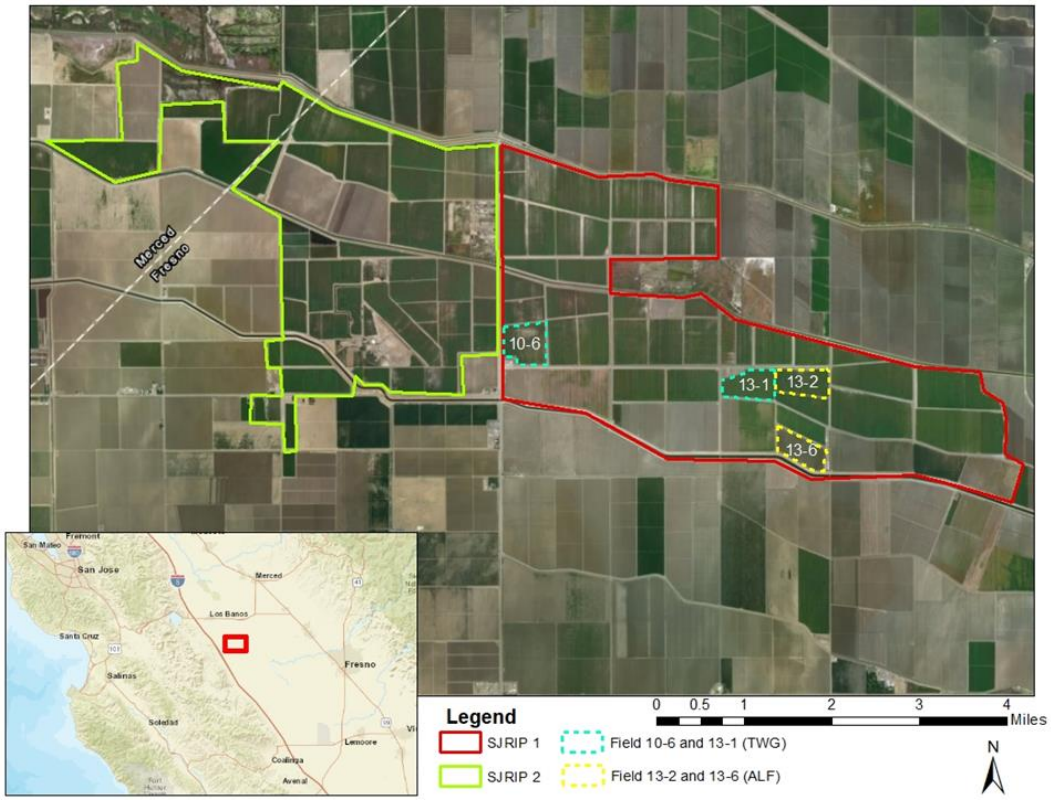

Figure 2. The San Joaquin River Improvement Project (SJRIP) receives subsurface tile drainage from 44,000 hectares of selenium-impacted agricultural land, including the Panoche Water District and adjacent water districts on the westside of the San Joaquin Valley.

2.2. Selected Fields

Four forage fields were selected for the study. The fields were chosen based on the availability of historical data on irrigation diversions, and the forage yield collected at each cutting. As shown in Figure 2, fields 13-2 and 13-6 were planted with alfalfa (ALF), and fields 13-1 and 10-6 were planted with 'Jose' tall wheatgrass (TWG). Fields 13-1 and 13-2 had subsurface drains, whereas 10-6 and 13-6 had no subsurface drainage system. TWG field 10-6 was one of the original fields in the SJRIP; its saline irrigation began in 2001. Fields 13-1, 13-2 and 13-6 were developed in 2004; thus, all of the fields in this study had been irrigated with saline drainage water, blended with less saline water in the case of ALF fields, for more than twelve years. In the county soil survey, all four fields were mapped as clays, belonging to the Chateau (10-6), Deldota (13-1), Tranquillity and Deldota (13-2), and Tranquillity (13-6) soil series.

2.3. Irrigation Data

The salinity of the canal diversions into the four selected forage fields was measured using InSitu electrical conductivity (EC) sondes, which were installed to provide hourly measurements of the salinity of the applied irrigation water (Figure 3) and the depth of the water in the irrigation supply ditches. The water depth provides an indicator that irrigation is most likely taking place, when water levels rise to a point where the siphon tubes that divert water into each field can be operated. The water depth provides a check on the accuracy of written records provided by the water district. A limited number of grab samples were also collected for chemical composition, and were sent to the California Department of Water Resources' designated laboratory for the analysis of their chemical constituents. The samples were filtered through a 0.22 m pore size nylon filter (Fisherbrand 25 mm syringe filter; Fisher Scientific, Tustin, CA, USA) prior to chemical analysis, and the portion used for analysis of Na^+, Ca^{2+}, Mg^{2+} and B was acid fixed using 1 mL of 70% nitric acid. Chloride and $SO_4{}^{2-}$ were measured using a Dionex DX-500 ion chromatography instrument (IC; Sunnyvale, CA, USA) according to EPA method 300.0 [17]. Sodium, Ca^{2+}, Mg^{2+} and B were measured using inductively coupled plasma atomic emission spectrometry (ICP-AES) according to EPA method 200.7.

Figure 3. EC sondes installed at each field inlet for the real time monitoring of the salinity and water depth in the supply ditch. The daily irrigation application volumes were supplied by the water master at Panoche Water District. The images show the supply ditch and gated pipe installations of the In-Situ sondes, which are capable of reading EC, temperature and pressure (the depth of the water in the ditch).

2.4. Soil Salinity Surveys Using the EM38-MK2

In this study, soil salinity surveys were performed to determine the levels and the spatial and temporal variability of the salinity in the four forage fields. The surveys were carried out with a Geonics

Ltd. (Mississauga, ON, Canada) EM38-MK2 electromagnetic induction sensor. The electromagnetic induction (EM) technique behind this sensor has been widely employed by soil scientists to better understand the spatial variability of soil properties at the field and farm scales. It is a reliable, quick, and easily mechanized technique for collecting salinity data as compared to the more traditional sampling method using a hand auger. EM instruments have been used to map soil moisture content [24] soil texture [25], clay content [26] and soil salinity [27,28]

The EM38-MK2 sensor provides simultaneous measurements of the soil's apparent electrical conductivity (EC_a) at two profile depths: 0.75 m and 1.5 m. The EM38-MK2 and a GPS unit (Trimble, Sunnyvale, CA, USA) were connected to the serial ports of an Allegro-CX portable field device (Juniper Systems; Logan, UT, USA) for downloading the EM and GPS measurements. Custom software for the Geonics EM38-MK2 was installed on the Allegro-CX to facilitate the data logging. The EM-38-MK2 was mounted on a non-conductive PVC sled and dragged behind an all-terrain vehicle (ATV) to perform the salinity surveys (Figure 4). The GPS unit was placed on the ATV to record the geographical coordinates of the EM measurements.

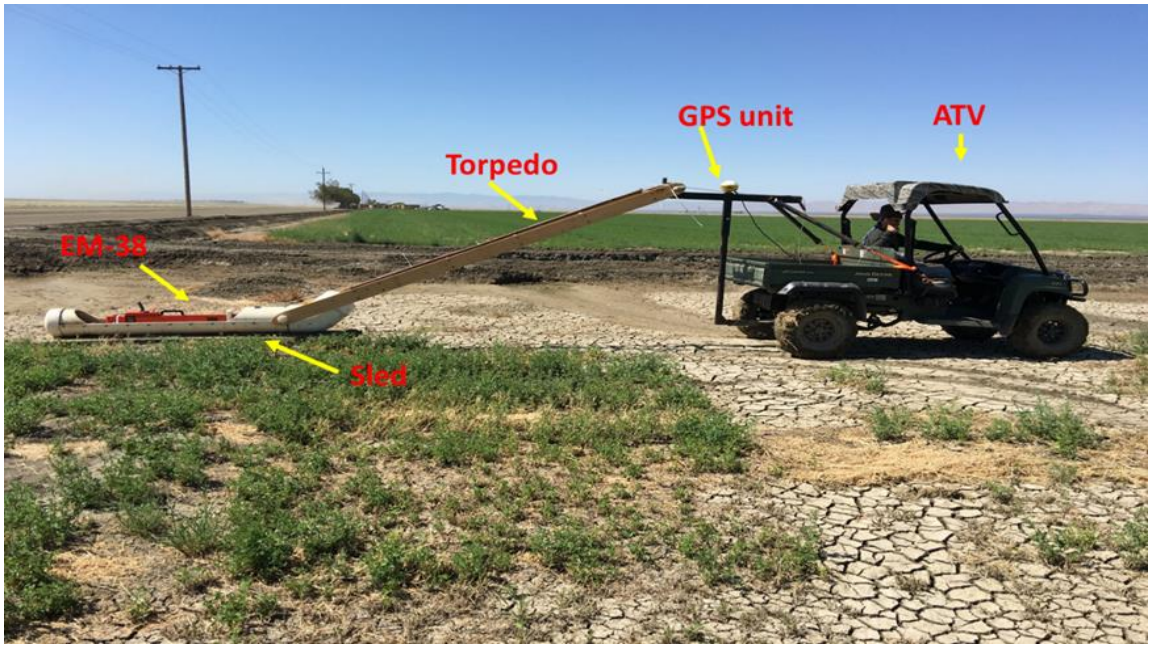

Figure 4. General setup for the soil salinity surveys using the GPS unit and the Geonics EM38-K2 mounted on a PVC sled and dragged behind an ATV. The gantry that connected the ATV to the sled was made entirely of fiberglass, in order to avoid electromagnetic interference.

Salinity surveys were performed for each field during the spring and fall seasons of 2016 and 2017, following the methods described by [29,30]. Before beginning the surveys, the EM38-MK2 was mounted at a height of approximately 1.5 m above the ground using a PVC stand, and was calibrated following the manufacturer's guidelines. The ATV was navigated along transects marked with flags placed 30 m apart. The speed of travel varied from 8 to 9.7 km hr^{-1}, and the average distances between two consecutive survey sites are given in Table 1. All salinity surveys were conducted 3 to 5 five days after the irrigations were completed, and when the soil moisture contents were close to the field's capacity. For each field, survey measurements were initiated 5 to 10 m into the field on all sides to avoid any edge effects.

Table 1. EM38 soil survey information for surveys in the spring and fall of 2016 and 2017 in two tall wheatgrass (TWG) fields (10-6 and 13-1) and two alfalfa (ALF) fields (13-2 and 13-6). The fields were 35.6 ha (10-6), 70 acres (13-1) and 30 ha (13-2 and 13-6).

Field	Date		Number of Transects		No. of Survey Sites within Field		Avg. Distance between Sites (m)	
	Spring	Fall	Spring	Fall	Spring	Fall	Spring	Fall
2016								
10-6 (TWG)	May	October	21	23	5785	5101	1.9	2.3
13-1 (TWG)	May	October	18	24	3812	3488	1.5	2.4
13-2 (ALF)	June	September	19	20	3515	3625	1.8	1.8
13-6 (ALF)	June	September	24	26	4283	4038	1.8	2.1
2017								
10-6 (TWG)	April	October	21	22	4366	4346	2.5	2.6
13-1 (TWG)	April	September	28	27	4533	3399	2.1	2.6
13-2 (ALF)	May	September	28	28	3816	3076	2.3	2.8
13-6 (ALF)	April	September	24	24	2900	2815	2.7	2.8

2.5. Soil Sampling Locations (Ground-Truthing)

After completing the EM38 motorized surveys, the ESAP-RSSD program was used to determine the soil sampling locations, following a statistical sampling design that selects uniformly across the sample frequency distribution, and is based on the range and variability of the EC_a data collected [31,32]. In our study, twelve sample locations were selected across each surveyed field. Soil samples were collected either immediately after the soil surveys were completed or the next morning, in order to ensure that the soil conditions had not changed. Any dry or loose soil (if present at the soil surface) was removed, since it would not be reflected in the EC_a measurements because of its low moisture conditions. At each sampling site location, soil was taken at 30 cm depth increments across 0–120 cm with a hand auger. The soil samples were labeled and stored in zip-lock bags. For each survey, 48 samples were collected for lab analyses.

2.6. Soil Analysis

One portion (50–70 g) of the ground-truth soil sample was dried in an oven at 105 °C for 3–4 days in order to calculate its gravimetric water contents. The other portion was dried in a 55 °C oven and ground using a mechanical pulverizer to pass it through a 2 mm sieve. Saturated soil pastes were prepared with deionized water using 200 g of 55 °C dried soil, and were allowed to stand overnight prior to vacuum filtration [33]. The saturation percentage (SP) was calculated as the weight of the water required to saturate the soil divided by the weight of the dry soil used to prepare the saturation paste, with the decimal fraction converted to a percentage. The soil salinity (EC_e) was measured from the paste extracts using an EC meter (AccumetTM Basic AB30 Conductivity meter, Fisher scientific, Leicestershire, England). The pH of the saturated soil paste extracts was measured using a pH/conductivity meter. In fall 2017, the ground-truth soil samples collected at a 0–30 cm depth were also analyzed for boron (B), calcium (Ca^{2+}), magnesium (Mg^{+}), sodium (Na^{+}), chloride (Cl^{-}) and sulfate (SO_4^{2-}). These additional analyses performed on the saturated past extracts of the samples collected in the soil top layer provided a good representation of the important chemical properties in the crop root zone. Sodium adsorption ratios (SAR) were then calculated from the Ca^{2+}, Mg^{+} and Na^{+} values.

2.7. EC_a to EC_e Calibration and Spatial Maps

For each survey, the ESAP-Calibrate program was used to convert the EC_a readings into EC_e etimates using spatially referenced multiple linear regression models [31]. The DPPC (dual pathway parallel conductance) correlation analysis was performed, where a set of EC_a readings (referred as Calc EC_a) were estimated based on the measured salinity (EC_e), SP and water content values using Rhoades' equation [31,34]. This analysis provided a theoretical value for the EC_a readings at each sampling point, and served as a quality control check. Correlations between the calculated EC_a, measured EC_a, EC_e, and other soil variables collected were also performed. Finally, a spatially referenced regression

model was generated to predict the logarithm of the salinity levels ($lnEC_e$) at each sampling site and depth within the surveyed area.

Maps depicting the spatial distribution of the salts within each field were developed using ESRI's ArcGIS Pro 2.3.1. Maps were created for each sampled depth, as well as for the average salinity across the soil profile (0–120 cm) using satellite imagery as their base-maps. The Inverse Distance Weighing (IDW) technique, a deterministic geostatistical method of interpolation, was used for the interpolation of the data, and was provided by the Spatial Analyst toolbox within ArcMap. This method was selected, instead of commonly used geospatial methods such as kriging, because of the high spatial resolution of the survey data collected. A fixed radius setting of 40 m was used to generate the interpolated data with a minimum of 25 sample points. The output cell size that determined the map grids was 5 m.

2.8. Leaching Fraction Estimation

The leaching fraction (LF) can be estimated by assuming steady-state conditions and good drainage as follows:

$$LF = (Cl_{iw})/(Cl_{d,[x,y]}) \text{ or } (EC_{iw})/(EC_{d,[x,y]})$$

where Cl_{iw} or EC_{iw} represents the chloride or salinity value for the irrigation water, and the denominators represent the depth and location-specific predictions of the chloride or EC of the water (drainage) moving below the root zone. For our LF calculation, the average irrigation water salinity for the irrigation season (2016 or 2017), obtained from the EC sondes installed in each field, was used for the numerator. For the denominator, the EC of the soil water (EC_{sw}) was considered as the best estimate of the EC of the drainage. Rather than using the standard multiplication factor of the two to convert EC_e to EC_{sw}, the EC_e of the ground-truth samples was multiplied by the water content ratio (W_{sp}/W_f) using the saturated paste water content (W_{sp}) and the field water content of the ground-truth samples (W_f) on a gravimetric basis. For each field and soil survey, LFs were estimated for each 30 cm soil layer and for the entire soil measurement zone (0–120 cm).

2.9. Forage Sampling and Analysis

Twelve forage tissue samples were collected from 1 m^2 areas in each field prior to harvest during the period of April to July in 2017. The herbage was cut at the top of the crown at the sites where the soil samples were collected during the spring EM38 surveys. Field samples were taken to the laboratory, where the fresh weight of the biomass was measured. The samples were rinsed with deionized water to remove any surface salt and dust, and then dried for 2–3 days in a forced air oven at 50 °C to obtain the dry weight. The dried samples were then ground in a mechanical grinder to pass a 40-mesh screen for subsequent analyses of potassium and sodium in the shoots. The K^+ and Na^+ contents in the forage shoot tissues were determined using an Agilent 240AA Atomic Absorption and Emission Spectrophotometer (Agilent; Santa Clara, CA, USA). The K^+ and Na^+ elements were analyzed in the absorption and emission modes, respectively. The tissue extraction consisted of 0.5 g of dried and ground shoot sample mixed with 30 mL of a 2% acetic acid. The extracts were filtered through a #1 filter paper to remove any particulates.

3. Results and Discussion

3.1. Irrigation Water

In general, the irrigation waters for the forage fields, as analyzed from the grab samples, were alkaline, averaging a pH of 7.7 to 8.0, and relatively high in bicarbonate (72–150 mg L^{-1} averages for the four fields). The salinity was more sulfate ion-dominated when compared to the concentrations of chloride and sodium ions in solution. As the salinity increased, the sodium adsorption ratio (SAR) and boron concentrations also increased (Table 2). The EC_{iw} data for grab samples are shown in Table 2, but they represent a very limited number of samples; thus, the discussion of the salinity of the

irrigation water applied to the forage fields will focus on the EC sonde (continuous monitoring) data described below.

Table 2. Chemical composition of the saline drainage water used to irrigate tall wheatgrass (TWG) and alfalfa (ALF) fields in 2016 and 2017. The data are for grab samples taken periodically for chemical analysis.

Sampling Month	EC_w [1] (dS/m)	pH	SAR [2]	Boron (mg/L)	Ca^{2+}	Mg^{2+}	Na^+ (mmol/L)	Cl^-	SO_4^{2-}	HCO_3^- (mg/L)	CO_3^{2-} (mg/L)
Field 10-6 (TWG)											
Aug. 2016	4.5	8.3	1.2	3.7	5.1	.	.	17.0	26.5	145	3
Sept. 2016	6.9	8.1	12.6	15.2	15.7	14.8	49.0	36.2	39.0	124	2
April 2017	5.7	7.9	9.5	9.6	16.9	9.0	34.2	20.1	35.4	177	1
May 2017	5.2	7.8	10.4	12.5	19.8	12.0	41.5	13.8	20.8	155	<1
Sept. 2017	3.3	7.8	7.8	5.3	9.0	5.6	21.2	10.7	20.4	113	<1
Average	**5.1**	**8.0**	**8.3**	**9.3**	**13.3**	**10.3**	**36.5**	**19.6**	**28.4**	**143**	.
Field 13-1 (TWG)											
Aug. 2016	3.2	7.8	5.0	2.2	4.1	2.7	9.3	10.6	19.9	137	1
Sept. 2016	0.4	7.2	4.6	3.5	19.7	10.8	17.8	14.9	28.1	170	1
April 2017	9.2	8.1	12.4	14.4	18.3	12.6	48.7	30.6	45.0	191	2
June 2017	2.9	7.8	4.2	2.9	17.8	9.7	15.4	14.9	26.4	161	1
Sept. 2017	3.6	7.6	4.9	3.3	15.4	8.7	16.9	13.5	25.0	150	<1
Average	**3.9**	**7.7**	**6.2**	**5.3**	**15.0**	**8.9**	**21.6**	**16.9**	**28.9**	**162**	.
Field 13-2 (ALF)											
Aug. 2016	1.0	8.4	4.2	0.94	2.1	1.5	5.6	3.1	4.6	76	2
Sept. 2016	0.7	7.9	3.5	0.73	2.1	1.8	4.8	3.3	3.2	85	1
Sept. 2017	0.6	7.2	2.4	0.60	1.3	1.0	2.6	1.0	2.4	55	<1
Average	**0.8**	**7.8**	**3.4**	**0.76**	**1.8**	**1.4**	**4.3**	**2.5**	**3.4**	**72**	.
Field 13-6 (ALF)											
Aug. 2016	3.9	8.2	2.8	1.08	8.7	5.0	7.4	15.6	24.7	160	3
Sept. 2016	0.4	7.7	4.0	2.58	18.0	9.1	14.5	13.5	24.6	151	1
April 2017	3.4	7.8	4.0	2.80	16.9	8.9	14.4	11.9	24.4	146	<1
May 2017	3.0	7.8	4.4	3.00	17.9	9.8	16.2	14.0	28.6	142	<1
Sept. 2017	3.7	7.8	4.1	2.50	16.6	9.3	14.9	13.5	25.0	152	<1
Average	**2.9**	**7.9**	**3.8**	**2.39**	**15.6**	**8.4**	**13.5**	**13.7**	**25.5**	**150**	.

[1] EC_w = electrical conductivity (salinity) of applied irrigation water; [2] SAR = sodium adsorption ratio. Unit-less.

The sonde data provided EC values from the continuously monitored diversion sites and gave a good representation of the salinity of the drainage waters applied as irrigation to the forage fields (Figure 5). The TWG fields were irrigated with higher salinity water (1.2–9.3 dS m^{-1}) compared to the ALF fields, which were irrigated with lower salinity water (0.5–6.9 dS m^{-1}), reflecting the lower salt tolerance of alfalfa compared to tall wheatgrass. In Figure 5, the salinity of the irrigation water (EC_{iw}) applied to each field between 1 July 2016 and 25 October 2017 is reported as daily means, which averaged 5.6 and 4.8 dS m^{-1} for TWG fields 10-6 and 13-1, and 2.0 and 3.7 dS m^{-1} for ALF fields 13-2 and 13-6, respectively. For the ALF fields, data were more limited in 2016 compared to 2017. Alfalfa field 13-2 received high quality irrigation water (EC_{iw} < 1dS m^{-1}) for most of the year in 2017, whereas between August and November 2016, the irrigation water salinity was often in the 3–4 dS m^{-1} range.

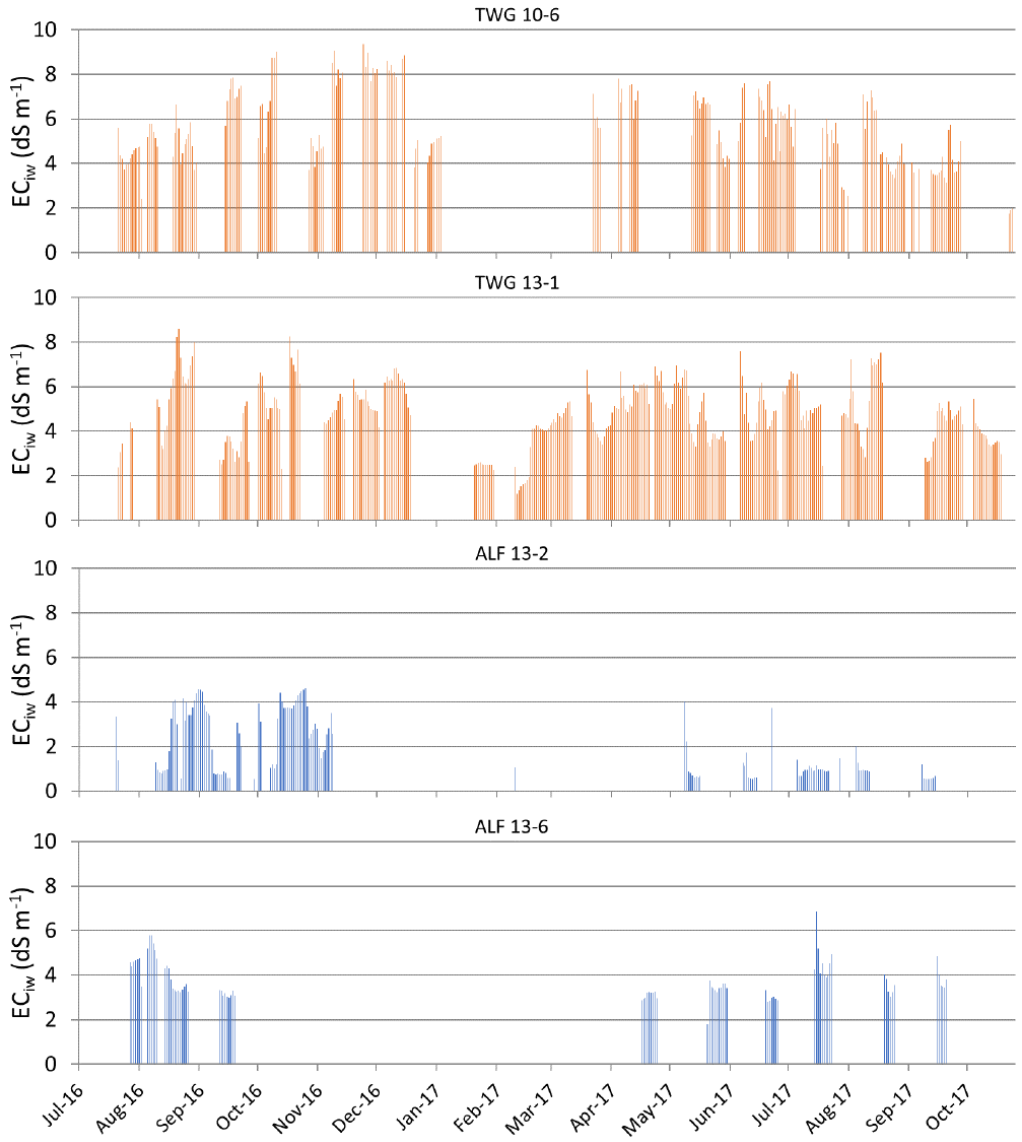

Figure 5. Mean daily irrigation water salinity (EC_{iw}) of the saline drainage water used to irrigate tall wheatgrass fields 10-6 and 13-1 (upper two graphs), and alfalfa fields 13-2 and 13-6 (lower two graphs) in 2016 and 2017. In-SITU Series 200 sondes were used to monitor the EC and water depth in each supply ditch.

3.2. Soil Chemistry

The chemical analyses performed on the saturation paste extract of the ground-truth soil samples collected at 0–30 cm depth during the fall 2017 surveys indicated that the soils in the TWG fields had sodium adsorption ratios (SAR) roughly twice as elevated as those observed in the ALF fields (Table 3). The high mean SAR values of 20.8–22.1 obtained in the TWG fields would suggest low water infiltration into the soil; however, this was not observed in the two TWG fields, possibly due to the fibrous root system of the forage, which help improve infiltration. The soil mean boron concentrations were also much higher in the TWG fields (18.9–21.9 mg L^{-1}) compared to the ALF fields (4.0–11.4 mg L^{-1}). Although such elevated levels would be detrimental to the growth of most other crops, growth hindrance was not observed in the TWG fields. Thus, these findings reflect the high salt and boron tolerance of 'Jose' tall wheatgrass when grown using saline drainage water, as observed by [7]. Na+ was the predominant cation, in particular in the more saline TWG fields (10-6

and 13-1). The soil salinity in this area had a high sulfate component, as evidenced by the soil sulfate concentrations, which were similar to the chloride concentrations.

Table 3. Soil chemical properties of the saturated soil paste extract for EM38 ground-truth samples (0–30 cm depth) taken in tall wheatgrass fields (10-6 and 13-1) and alfalfa fields (13-2 and 13-6) in fall 2017. Fields 13-1 and 13-2 were drained, and 10 -6 and 13-6 were undrained fields.

	Field 10-6		Field 13-1		Field 13-2		Field 13-6	
	Mean	Range	Mean	Range	Mean	Range	Mean	Range
EC_e [1] (dS m^{-1})	15.2	3.8–25	18.9	13.5–25.1	13.3	9.9–16.3	10.5	6.4–14.3
SP [2] (%)	53.8	62.7–156	83.5	75.5–92.6	84.6	70.9–114	72.5	52.6–85.5
SAR[3]	22.1	8.7–38.1	20.8	15.3–30.0	10.7	4.9–15.5	7.6	4.9–11.5
B (mg L^{-1})	21.9	4.1–38.5	18.9	12.7–26.7	11.4	5.4–19.1	4.0	2.1–7.0
Ca^{2+} ($mmol_c$ L^{-1})	12.0	3.6–17.8	12.7	12.2–13.3	12.7	11.8–15.6	14.5	11.7–16.6
Mg^{2+} ($mmol_c$ L^{-1})	14.9	2.2–31.7	15.5	12.4–18.9	7.3	6.4–9.6	8.1	5.8–10.2
Na^{+} ($mmol_c$ L^{-1})	122.9	21.2–272	111.3	76.7–168.6	48.7	21.5–69.0	36.9	20.8–59.2
Cl^{-} ($mmol_c$ L^{-1})	63.3	6.5–147	51.6	29.0–76.4	.	.	25.5	8.2–39.8
SO_4^{2-} ($mmol_c$ L^{-1})	53.1	9.8–112	53.5	43.0–67.6	36.5	26.0–47.0	25.4	19.7–31.7

[1] EC_e = electrical conductivity of a saturation soil paste extract; [2] SP = saturation percentage.

3.3. Soil Survey Quality Checks and Calibration of EC_a to EC_e

The analysis of the soil salinity survey data using the ESAP-Calibrate program revealed correlations of >0.90 between the EM_h (horizontal) and EM_v (vertical) measurements, suggesting that there were no moisture or textural irregularities in the soil profile. The surveys were conducted when the volumetric water content of the soil was at least 70% of field capacity. The soil water content relative to the field capacity was estimated by ESAP based on Rhoades equations [31,34], and it was observed that the surveys were conducted when the volumetric water content of the soil was at least 70% of field capacity (data not shown). Results from the data quality check performed on the acquired EC_a measurements for each salinity survey are presented as DPPC correlations in Table 4. These correlations show the relationship between the log of 'CalcECa' (calculated ECa) and the z1 signal (EM data), averaged over the entire soil profile [31]. Poor correlations were observed for only one field, TWG 13-1, during the fall seasons. Such results could be explained by the large size of the field and/or the high soil moisture variability across the field and the profile depth. An extended period (up to 5 days) was required to complete one full irrigation cycle; therefore, the most recently-irrigated portion of the field may have been above field capacity when the survey was conducted, whereas the first irrigated section was drier.

Table 4. DPPC (Dual pathway parallel conductance) model correlations that describe the relationship between the log of 'CalcECa' (calculated ECa) and the z1 signal (EM data), and serve as a quality check for the ECa data collected during EM38 soil surveys.

	Spring 2016	Fall 2016	Spring 2017	Fall 2017
10-6 (TWG)	0.977	0.966	0.899	0.897
13-1 (TWG)	0.868	0.216 [1]	0.878	0.536 [1]
13-2 (ALF)	0.905	0.788	0.949	0.812
13-6 (ALF)	0.79	0.844	0.963	0.917

[1] Values indicate a less than desirable correlation with the theoretical model.

After the data quality checks, linear regression models were developed, and those that produced the best predictions of the (log) salinity level at each surveyed point were selected. The best-fit regression models developed for each survey are shown in Table 5, in which:

- b0, b1, b2, b3 and b4 are the regression parameters;
- z1 and z2 are the transformed and de-correlated EM signal readings (i.e., vertical 1.5 m and horizontal 0.75 m);
- x and y are the centered and scaled location coordinates.

Table 5. Multiple linear regression models used to convert ECa data measured by the EM38 to soil salinity (EC_e), with the model R-square values to show the goodness of fit. The regression equations are for soil surveys conducted in tall wheatgrass (TWG) and alfalfa (ALF) fields. An F-test (significance statistic in the footnote) was used to identify the model that best fits the population from which the data were sampled.

	Field	MLR Model Used	R-Squared (Averaged over 0–120 cm)
Spring 2016	10-6 (TWG)	ln(ECe) = b0 + b1(z1) + b2(z2)	0.910 [1]
	13-1 (TWG)	ln(ECe) = b0 + b1(z1) + b2(y)	0.784 [1]
	13-2 (ALF)	ln(ECe) = b0 + b1(z1)	0.837 [1]
	13-6 (ALF)	ln(ECe) = b0 + b1(z1)	0.550 [1]
Fall 2016	10-6 (TWG)	ln(ECe) = b0 + b1(z1) + b2(z1^2) + b3(x)	0.948 [1]
	13-1 (TWG)	ln(ECe) = b0 + b1(z1) + b2(z2) + b3(z1^2) + b4(x)	0.827 [1]
	13-2 (ALF)	ln(ECe) = b0 + b1(z1)	0.436 [2]
	13-6 (ALF)	ln(ECe) = b0 + b1(z1) + b2(z2)	0.846 [1]
Spring 2017	10-6 (TWG)	ln(ECe) = b0 + b1(z1)	0.793 [1]
	13-1 (TWG)	ln(ECe) = b0 + b1(z1) + b2(z2)	0.847 [1]
	13-2 (ALF)	ln(ECe) = b0 + b1(z1) + b2(z2) + b3(y)	0.956 [1]
	13-6 (ALF)	ln(ECe) = b0 + b1(z1) + b2(z2)	0.960 [1]
Fall 2017	10-6 (TWG)	ln(ECe) = b0 + b1(z1) + b2(z2)	0.831 [1]
	13-1 (TWG)	ln(ECe) = b0 + b1(z1) + b2(z2)	0.507 [2]
	13-2 (ALF)	ln(ECe) = b0 + b1(z1) + b2(y)	0.609 [2]
	13-6 (ALF)	ln(ECe) = b0 + b1(z1) + b2(x) + b3(y)	0.929 [1]

[1] Significant at $p \leq 0.01$. [2] Significant at $p \leq 0.05$.

3.4. Soil Salinity Derived from the ESAP Calibration Software and Leaching Fraction (LF)

The ground-truth soil salinity (EC_e) data for all fields, sampling times and profile depths are shown in Table 6. With the exception of TWG field 10-6, there was little or no increase in soil salinity in the forage fields between spring and fall in 2016. This could be explained by a lack of rainfall in the winter of 2016, such that the irrigation applications during the summer helped to leach some of the salts below the 120 cm soil profile depth. In 2017, there was also relatively little increase in the soil salinity from spring to fall. The field with the highest soil salinity was TWG field 13-1, which exhibited mean levels between 16.4 and 19.3 dS m^{-1} EC_e across the 0–120 cm soil profile. The highest salinity levels were observed at the lower sampled depths (90–120 cm), with mean EC_e values ranging from 19 to 23 dS m^{-1}. Field 13-1 was drained, and there was evidence of leaching, given that, in all four sampling periods, the soil salinity was lowest in the 0–30 cm soil depth interval and highest in the 90–120 depth interval. The leaching fraction (LF) data (Table 7) also show that leaching was greatest in the surface layer (15.2–19.7%) and lowest in the 90–120 cm soil layer (9.4–11.5%) for this field. TWG field 10-6 was less saline, with average measured salinity for the 0–120 cm soil profile ranging from 12.5 to 16.8 dS m^{-1} EC_e over the two-year period (Table 6). Although it was an undrained field, the salinity was relatively uniform, and the depth in this profile and estimated LF's were highest for this field, being 21 to 36% over the two-year period (Table 7). Field 10-6 was one of the earliest fields brought under saline irrigation in the SJRIP, and thus, after more than fifteen years of saline irrigation, it had likely reached equilibrium conditions with respect to salt dissolution and precipitation within the soil profile.

Table 6. Average soil salinity EC_e (dS/m) and range derived from ESAP calibration software for each 30 cm increment and the entire 0–120 cm soil depth based on soil samples taken at twelve ESAP-directed locations per field. The data are for surveys taken in tall wheatgrass (TWG) and alfalfa (ALF) fields in the spring and fall of 2016 and 2017.

Depth (cm)	EC_e (dS/m)							
	Spring 2016		Fall 2016		Spring 2017		Fall 2017	
	Mean	Range	Mean	Range	Mean	Range	Mean	Range
10-6 (TWG)- *not drained*								
0–30	10.6	2.5–23.3	15.5	3.2–34.0	11.8	4.1–19.0	14.6	3.3–38.2
30–60	13.9	3.2–27.3	17.0	1.7–32.4	14.8	5.1–23.9	16.5	5.8–33.4
60–90	12.2	3.1–23.3	18.1	1.4–28.1	15.6	5.6–25.0	16.4	6.0–28.8
90–120	12.7	3.0–26.0	16.7	1.1–27.0	15.2	5.7–23.8	14.8	4.4–27.5
0–120	**12.5**	**2.5–27.3**	**16.8**	**1.1–34.0**	**14.4**	**4.1–25.0**	**15.7**	**3.3–38.2**
13-1 (TWG)- *drained*								
0–30	13.0 [1]	10.3–17.3	12.6	6.8–40.7	12	6.1–17.7	13.4	9.5–16.6
30–60	19.6	13.2–33.3	17.0 [1]	9.1–31.0	16.3	7.2–25.1	19.6	14.2–25.4
60–90	20.8	15.1–31.4	17.5	11.4–45.5	18.5	9.3–27.1	20.3 [1]	14.9–26.0
90–120	23.2	18.6–29.8	19.2	8.2–47.9	18.6	9.6–26.4	21.0 [1]	16.1–25.0
0–120	**19.3**	**10.3–33.3**	**16.6**	**6.8–47.9**	**16.4**	**6.1–27.1**	**18.6**	**9.5–26.0**
13-2 (ALF)- *drained*								
0–30	9.6	3.3–17.1	8.0	4.7–10.2	7.0	2.3–13.4	7.0	3.6–10.4
30–60	14.0	6.7–21.2	12.0	7.4–15.1	11.5	3.8–22.0	13.7 [1]	10.1–16.0
60–90	16.5 [1]	10.6–21.4	14.9	11.1–17.2	14.1	6.5–22.5	16.2 [1]	13.6–17.8
90–120	17.2	8.6–25.4	15.2 [1]	13.6–16.1	15.2	7.6–23.3	15.8	12.2–19.6
0–120	**14.4**	**3.3–25.4**	**12.6**	**4.7–17.2**	**12.0**	**2.3–23.3**	**13.3**	**3.6–19.6**
13-6 (ALF)- *not drained*								
0–30	5.7	3.0–9.5	7.2	4.3–10.9	5.1	1.8–14.6	6.9	4.5–9.9
30–60	8.9	5.0–14.2	10.3	6.3–15.5	9.9	3.3–27.0	10.6	6.0–17.4
60–90	10.8	7.6–14.3	12.1	8.5–15.6	12.0	5.8–22.8	12.2	6.5–18.3
90–120	10.3	6.7–14.4	11.0	6.5–16.4	10.8	6.6–17.4	11.8	7.1–16.2
0–120	**9.0**	**3.0–14.4**	**10.2**	**4.3–16.4**	**9.5**	**1.8–27.0**	**10.4**	**4.5–18.3**

[1] The highlighted values are where the R-square was not significant for the multiple linear regression model selected.

Table 7. Estimated leaching fraction (LF) for the 0–120 cm soil depth in tall wheatgrass (TWG) and alfalfa (ALF) fields in the spring and fall of 2016 and 2017. The LF was estimated as the ratio between the irrigation water salinity and the soil water salinity (EC_{iw}/EC_{sw}) for each 30 cm soil layer. The soil salinity (EC_e) from ESAP-directed soil sampling locations was used to calculate EC_{sw}.

Depth (cm)	Leaching Fraction (%)			
	Spring 2016	Fall 2016	Spring 2017	Fall 2017
10-6 (TWG)- *not drained*				
0–30	35.1	21.7	22.7	20.5
30–60	31.0	21.4	20.1	17.4
60–90	37.9	19.7	21.0	20.3
90–120	39.9	27.4	25.2	26.1
0–120	**36.0**	**22.6**	**22.2**	**21.1**
13-1 (TWG)- *drained*				
0–30	19.7	16.6	19.1	15.2
30–60	13.1	12.2	14.1	10.2
60–90	12.0	11.5	11.7	9.8
90–120	10.8	10.0	11.5	9.4
0–120	**13.9**	**12.6**	**14.1**	**11.2**
13-2 (ALF)- *drained*				
0–30	14.0	13.8	6.9	6.9
30–60	9.0	9.7	4.1	3.1
60–90	7.3	7.6	3.2	2.5
90–120	7.3	7.1	2.9	2.6
0–120	**9.4**	**9.5**	**4.3**	**3.8**
13-6 (ALF)- *not drained*				
0–30	29.7	22.2	38.7	25.5
30–60	21.5	17.3	19.8	16.6
60–90	18.6	14.8	15.4	14.1
90–120	21.1	18.3	16.4	15.6
0–120	**22.7**	**18.1**	**22.6**	**18.0**

The ALF fields (13-2 and 13-6) had lower soil salinity than the TWG fields (Table 6), which is consistent with the application of less saline water to the alfalfa fields compared to the tall wheatgrass fields. However, when comparing the alfalfa fields, the soil salinity was higher (12.0 to 14.4 dS m^{-1} ECe) across the 0–120 cm profile in field 13-2, which was irrigated with less saline water, especially in 2017 (Figure 5). Field 13-6, which was irrigated with more saline water, had lower soil salinity (9.0 and 10.4 dS m^{-1} EC_e) in the 0–120 cm layer. This discrepancy may be explained by the fact that field 13-2 had the lowest leaching fractions of all four fields (Table 7).

In the case of Field 13-2, which was drained, the soil salinity was lowest near the surface (0–30 cm depth) and increased with each depth increment in the soil profile. The leaching fraction data support this observation, with a higher estimated LF for the surface layer (7–14%) compared to the 90–120 cm soil layer (3–7%). Field 13-6 was not drained, but soil salinity was again lowest in the top 30 cm depth, and increased in the lower soil depth intervals between 60 and 120 cm. This is indicative of soil leaching and is, again, supported by the LF data showing greater leaching in the surface layer (22–39%) compared to the 60–120 cm soil layer (14–21%).

3.5. Leaching Fraction and Drainage through the Profile

As mentioned previously, the soil salinities (EC_e) were consistently lowest—and the leaching fractions were highest—in the surface layer (0–30 cm), and for the 60–120 cm soil depths, the soil salinities were higher and the leaching fractions were lower (Tables 6 and 7). This indicates downward salt displacement from the soil surface and is consistent with the relatively high levels of water application in this saline drainage water reuse site. Over the two-year period, the undrained fields (10-6 and 13-6) had much higher LF's (18–36%), and the two drained fields (13-1 and 13-2) had lower LFs (3.8–14.1%) for the 0–120 cm soil profile (Table 7). Generally, it would be expected that drained fields would have the higher LFs, but many factors influence the overall LF in a soil profile, including the irrigation volume and frequency, soil structure and texture, rooting depth and density, uptake of water from non-stressed portions of the crop root zone, salt precipitation and dissolution, and preferential flow [35–37]. For the four fields examined, applied water volume may have been an equally important factor influencing the extent of leaching in the 0-120 cm soil layer, as was the presence or absence of a drainage system. Alternatively, there is published evidence [36,37] that in undrained fields, crop water uptake may be reduced due to poor soil aeration, especially at salinities limiting crop growth. This would result in more water movement through the profile and could explain the higher LF measured for our undrained fields as compared to the drained fields

3.6. Spatial Variability in Soil Salinity

Figure 6 shows the salinity distributions across the soil profile (0–120 cm) at each ground-truthing location for all of the surveys. The salt distribution in field 10-6 (TWG) was highly variable among the twelve sampling locations, with EC_e values ranging from 1 to 32 dS m^{-1}. In addition, Figure 6 reveals that most of the salts were accumulating at the 30–60 cm and 60–90 cm soil depths, indicating a lack of adequate drainage, which was expected, as this field had no subsurface drainage system installed.

Spatial maps depicting the soil salinity distribution in field 10-6 are shown in Figure 7 for spring and fall 2017. The green and yellow areas represent lower soil salinity levels, and the orange, dull pink and white areas represent higher soil salinity. The maps illustrate that, throughout the study period, the western edge of field 10-6 had relatively lower EC_e values (<8 dS m^{-1}) compared to the central (8–18.5 dS m^{-1}) and eastern (>18.5 dS m^{-1}) parts of the field. This could be attributed to the textural variability of the soil within the field, as the western area was comprised of lighter-textured soil (as indicated by lower saturation percentage values). The maps show an increase in salinity from spring to fall 2017, and an accumulation of salt, primarily in the 30–60 cm and 60–90 cm depth ranges in both the fall and spring seasons. However, in fall 2017, the salt accumulation was also high in the surface 30 cm. Also shown on the upper maps are the transects/rows where the EC_a (mS/m) data were collected in the

field during the EM38-MK2 surveys, with the blue points representing the soil sampling sites. The EC_a data represent the averages of the vertical and horizontal EC_a measurements.

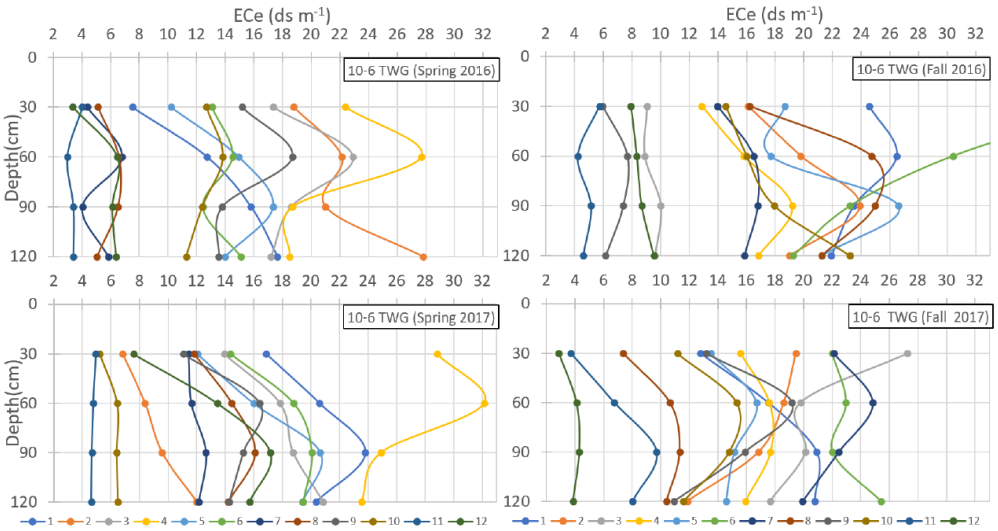

Figure 6. Salinity distribution in the soil profile at the 12 sampling locations in tall wheatgrass field 10-6 for the spring (left) and fall (right) surveys conducted in 2016 (upper) and 2017 (lower). Each line with data points represents one of the locations identified by the ESAP program based on the range and variability of the ECa data measured by the EM38. Sample number on the bottom legend corresponds to the location on the map for the respective season/year.

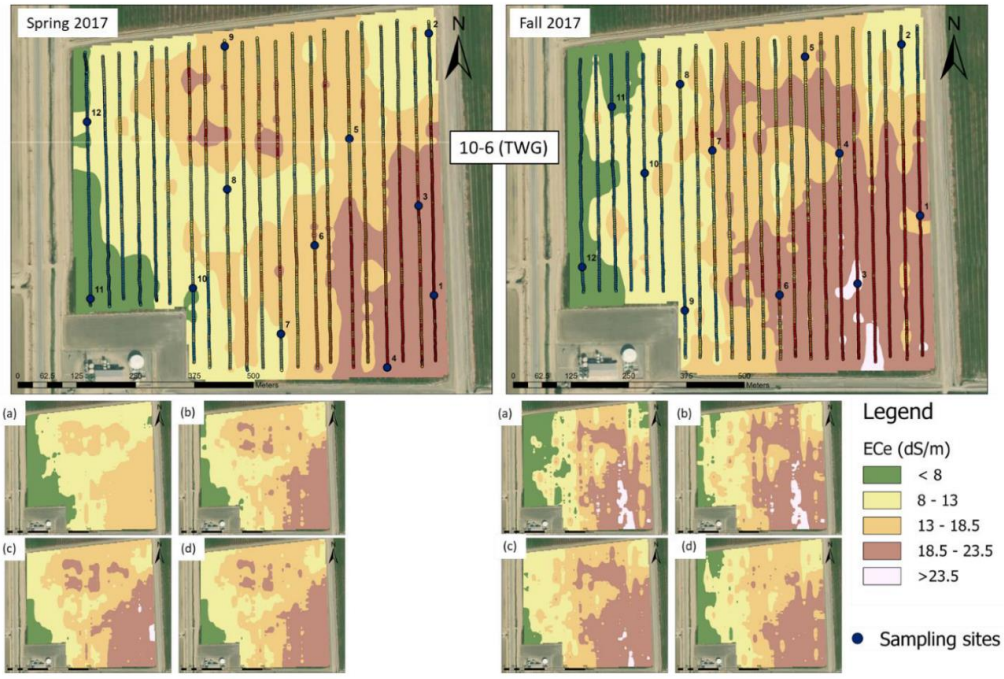

Figure 7. Spatial distribution of the average soil salinity for tall wheatgrass field 10-6 for the 0–120 cm depth (top two maps) and for each depth (bottom 8 maps): (**a**) 0–30 cm, (**b**) 30–60 cm, (**c**) 60–90 cm and (**d**) 90–120 cm. The data are for spring (left) and fall (right) 2017. The transects/rows where the ECa measurements were taken during the EM38-MK2 survey and the twelve ESAP-directed sampling locations are shown in the upper maps.

The soil salinity profiles for field 13-6 (ALF) for the two-year period are shown in Figure 8. Field 13-6 had the lowest salinity levels compared to the other fields, with soil salinity levels below

18 dS m^{-1} for almost all of the sampling locations and surveys. The most salt accumulation occurred within the 30–60 cm and 60–90 cm soil layers in 2016, as was observed in the other undrained field, 10-6. In the spring of 2017, two ground-truthing locations exhibited a soil salinity of 21–23 dS m^{-1}; however, these higher levels were no longer observed during the fall 2017 survey.

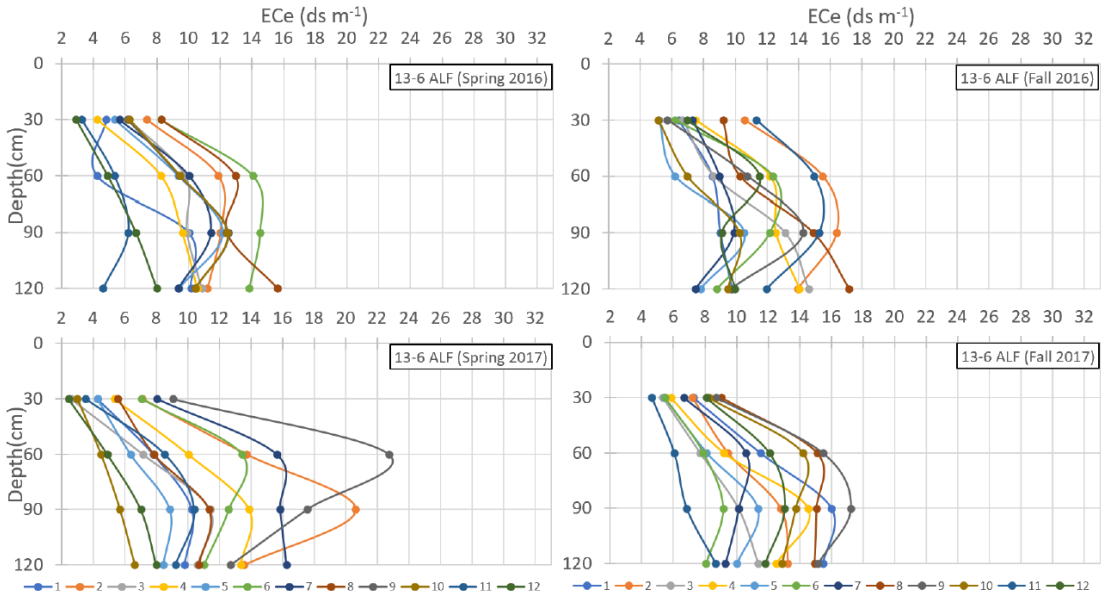

Figure 8. Salinity distribution in the soil profile at the 12 sampling locations in alfalfa field 13-6 for spring (left) and fall (right) surveys conducted in 2016 (upper) and 2017 (lower). Each line with data points represents one of the locations identified by the ESAP program based on the range and variability of the ECa data measured by the EM38. The sample number on the bottom legend corresponds to the location on the map for the respective season/year.

The spatial maps presented in Figure 9 show the lower salinity levels characteristic of ALF field 13-6 in 2017. Most of the surveyed field exhibited soil salinity lower than 13 dS m^{-1}. The salinity levels tended to increase from the spring to the fall, and most of the salts accumulated in the 60–90 cm and 90–120 cm depths. The maps also illustrate the lower variability in salinity across the field, as compared to 10-6.

For the other two fields 13-1 (TWG) and 13-2 (ALF), the salinity distribution profiles and spatial salinity maps are provided in Supplementary Materials. For Field 13-1 (TWG), it can be seen that leaching is greatest at the soil surface (Figure S1) and that in 2017, salinity was consistently higher in the western part of the field and in the 90-120 cm soil layer (Figure S2). It should also be noted that only a part of the field 13-1 was surveyed in spring 2016 due to high water content on the western portion of the field. The irrigation with siphon tubes progressed from east to west across each field, and the bank of siphon tubes deployed last was on the western side of the field. If inadequate time elapsed after the last irrigation event, the surface soils sometimes became waterlogged, which prevented the use of the ATV and risked damage to the crop along the tire tracks and path of the sled carrying the EM. During fall 2016, as previously reported, after performing the salinity survey of Field 13-1, the results showed poor DPPC correlations, which compromised the estimation of EC_e from EC_a.

Field 13-2 (ALF) consistently received good quality irrigation water, which produced a salinity profile indicative of relatively good leaching (Figure S3). This effect was evident during the fall of 2017, which showed a uniformly leached surface layer (Figure S4) in spite of the low leaching fraction (7–8%) estimated for this field (Table 7). Since this was a drained field, most of the salt accumulation was observed in the 90–120 cm soil depth, close to the subsurface tile drains. Only a portion of the field was able to be surveyed in year 2016 because of the high water content in the western section of the field at the time of the survey.

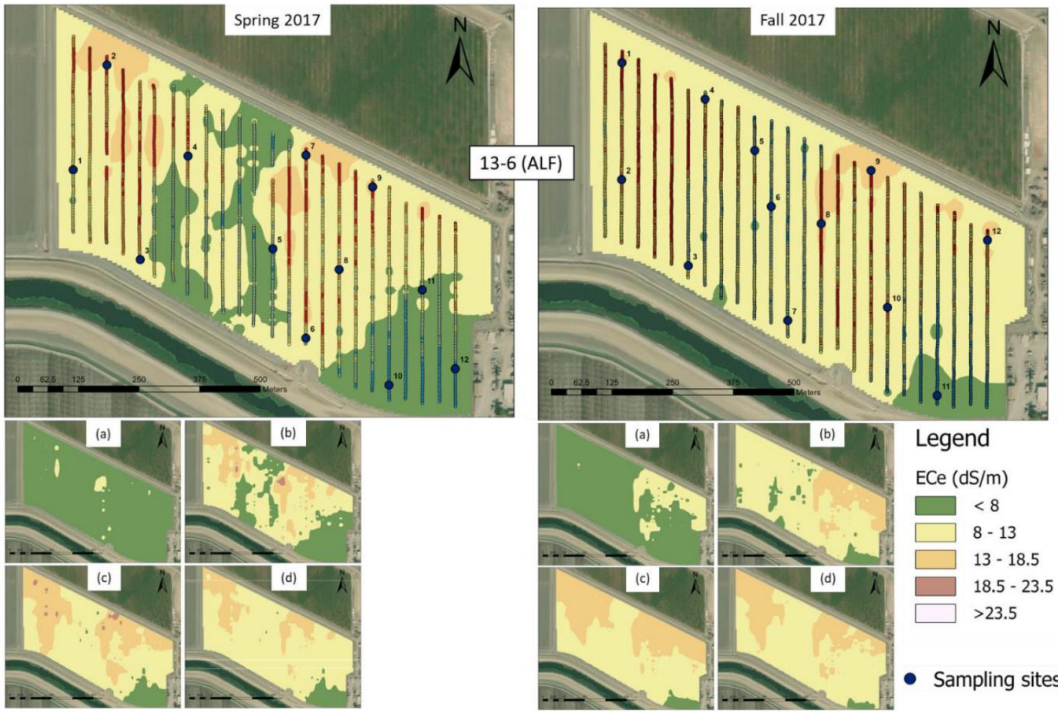

Figure 9. Spatial distribution of the average soil salinity for alfalfa field 13-6 for the 0–120 cm depth (top two maps) and for each depth (bottom 8 maps): (**a**) 0–30 cm, (**b**) 30–60 cm, (**c**) 60–90 cm and (**d**) 90–120 cm. The data are for spring (left) and fall (right) 2017. The transects/rows where the ECa measurements were taken during the EM38-MK2 survey and the twelve ESAP-guided sampling locations are shown in the upper maps.

3.7. Forage Analysis

Figure 10 shows the results from the correlations between the forage dry weight and soil salinity (EC_e), and between the forage dry weight and Na concentrations in the shoots of each forage. The data were combined from the two corresponding to each forage, and the R square (R^2) and p value are also provided. In no case was forage dry weight strongly correlated with soil salinity (EC_e) or with shoot Na; however, the correlation between the forage dry weight and soil salinity was stronger for the alfalfa fields, reflecting its lower salt tolerance compared to tall wheatgrass.

The soil salinity was very high in the TWG fields, but even in the range of 15–20 dS m^{-1} EC_e where most of the data points fell, the soil salinity did not appear to be the main factor influencing the forage dry weight. However, the tall wheatgrass yields measured for the entire field were low (4.78 t ha^{-1} average for fields 10-6 and 13-1) (data not shown) compared to another saline-irrigated site where tall wheatgrass was grown at similarly high soil salinities [7]; thus, it is possible that, within this range of low yield, other site-specific factors such as soil moisture (water-logging) or weed pressure were influencing the forage dry weight. The main goal of forage production at the SJRIP is not high yield, but rather adequate growth to maintain high evapotranspiration (ET) for the maximum consumption (disposal) of saline drainage water.

Likewise, the Na concentration in the tall wheatgrass shoots, although high (6–8 g kg^{-1}), was not exerting a strong influence on the forage dry weight. It should be pointed out that the tall wheatgrass yields obtained in these fields, although low, are remarkable given the very high soil salinity (15–20 dS m^{-1} EC_e) and soil boron concentrations (18–22 mg L^{-1}). Tall wheatgrass was the forage of choice for this saline drainage water reuse site, as evidenced by the continued planting of TWG over the past 20 years as the site has increased in size to 2600 ha.

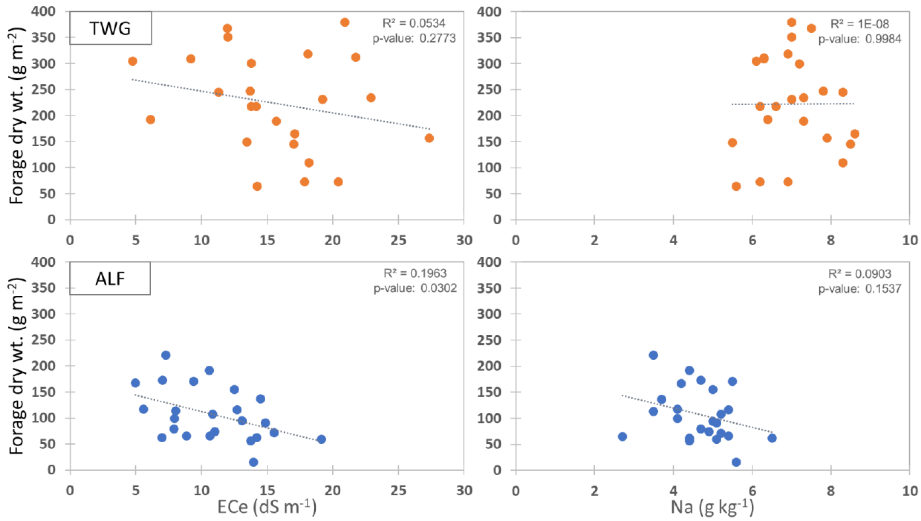

Figure 10. Scatterplots showing the relationship between the shoot dry weight and soil salinity (EC_e) (left) or sodium concentrations in shoots (right). The forage samples were taken between April and July 2017 from 1 m^2 areas corresponding to the twelve ESAP-guided soil sampling locations from the most recent EM38 survey. The data for tall wheatgrass (TWG) fields 10-6 and 13-1 were combined in each graph (top, orange), and data for alfalfa (ALF) fields 13-2 and 13-6 were combined in each graph (bottom, blue).

4. Summary

This paper highlighted the actions taken by stakeholders in the western San Joaquin Valley of California to sustain irrigated agriculture in light of policy-driven environmental regulation that initially focused on controlling the selenium contamination in the Grasslands Basin wetlands and selenium loading to the San Joaquin River. This paper argued that irrigation sustainability will require a greater understanding of local and regional salt balance, and the development of a new suite of science-driven decision support tools and practices to maintain the crop root zone soil salinity within salt tolerance guidelines. The paper also recommended greater effort to bridge the information and technology gaps between the complexity of the EM38-MK2 instrument and its reliance on statistically-based ground truthing and the laboratory analysis of soil samples, and the annual planning and day-to-day decision making of irrigators. The paper provided detail on the steps involved in making a typical EM38-MK2 survey that would be the underpinning for any longer-term 1-D transient salinity modeling effort, using the Panoche Water District SJRIP facility as an example. The same protocols and interpretative analysis could apply to any salinity-impacted agricultural drainage reuse system worldwide.

In the current study, four fields planted with 'Jose' tall wheatgrass (TWG) and alfalfa (ALF) were surveyed with an EM38-MK2 instrument to determine the spatial and temporal variability of the soil salinity at SJRIP. The TWG fields were irrigated with higher salinity water compared to the ALF fields, and the soil salinities averaged 12 to 19 dS m^{-1} EC_e for the 0–120 cm profile, with boron concentrations of 19–22 mg L^{-1} in the top 30 cm over the two-year period. The ability of 'Jose' tall wheatgrass to grow and consume saline drainage water through evapotranspiration under these high saline and high boron conditions makes this forage a very suitable candidate for saline drainage water reuse systems.

Field 13-2 (ALF) received relatively good quality irrigation water throughout the study period. Tile drained fields 13-1 (TWG) and 13-2 (ALF) had improved leaching, as most salt accumulation was found in the lower portion of the soil profile (60–90 and 90–120 cm soil depths). In comparison, field 10-6, which was not drained, had high salinity in the 30–60 cm layer, in addition to the 60–90 and 90–120 cm soil layers. Field 10-6 had the largest variability in areal salt accumulation, which could be attributed to the variability in its soil texture. Field 13-2 showed evidence of salt leaching, with the fall 2017 survey showing a uniformly leached surface soil layer, most likely the result of irrigation

applications of good quality water. Generally, for all of the fields except field 13-2, there was an increase in the soil salinity measured during the fall survey compared to the spring survey, which was expected because of the additional leaching potential of salts due to winter rains. The salinity did not decrease as much during 2017, given the relatively heavier precipitation during 2017. Additional years of data will be instructive to see if the same salinity trends repeat over time and will help improve the calibration of the CSUID model, which benefits from having large perturbations in the soil salinity signal.

The estimation of the soil salinity (EC_e) was compromised during the fall season of both years for fields 13-1 (TWG) and 13-2 (ALF), as suggested by poor DPPC correlations and poor R-squared values for the regression model used to convert the EC_a data to EC_e. These results were partially explained by the high clay content (based on higher SP values) and high spatial variability of soil texture in these fields, which likely affected the EC_a readings [29]. However, field 13-1 was also particularly difficult to survey to achieve optimal soil moisture conditions due to the irrigation schedule practiced by the water district, which, on some surveys, left a portion of the field with standing water. In general, the model R-squared values were high, and resulted in good model fit for the majority of cases, allowing the realistic estimation of the average salinity of the crop rootzone (0–120 cm). The ability to discern good data from bad is very important in order to maintain the utility of these soil salinity surveys, and to maintain the confidence of the water managers in the SJRIP. The more complex the technology, the greater the need for quality control and transparency. Methods that combine a greater connection to metrics the irrigators understand will help to bridge this gap.

5. Conclusions

Areal maps delineating the areas of high and low salinity in the fields chosen for this study in the SJRIP have proven to be useful to the managers of the facility in guiding future irrigation practices. These maps have been shared and discussed with Panoche Water District in two data meetings, and in a poster. These data, in combination with a record of the declining yields in the alfalfa fields, led to a decision to fallow fields 13-2 and 13-6 during 2018. The other significant product from this study was the establishment of a ground-truthing dataset for potential soil salinity assessment using remote sensing techniques [4]. High resolution ground-truthing data are often hard to obtain for such efforts. There is also a possibility that hyperspectral sensors may become a better platform for the assessment of soil salinity due to their capability to detect and map saline soils in more detail. Moreover, the 12 sampling locations established in each field could potentially serve as monitoring sites, given that the selected sites depict the full range of variability across the surveyed area—these sites could also be used as representative sites to monitor changes in the salinity levels in these fields over time. However, it should be noted that the main purpose of the sampling design was to optimize the parameter selection for the regression model for accurate salinity (EC_e) estimation, and not to provide a statistical analysis of the data collected as part of the salinity survey [32,38].

As demonstrated by the project, the use of the EM38-MK2 instrument could be part of a long-term monitoring strategy where the soil surveys conducted with this instrument could be used in combination with less time-intensive and easier-to-automate techniques like remote sensing as part of a long-term salinity management strategy. The project has shown that root zone salinity can change seasonally and between years, thus requiring that the salinity of subsurface drainage water used for irrigation be monitored, along with precipitation, in order to ensure that crop salinity thresholds are not exceeded with consequent declines in forage crop yield and profitability. Strategic reclamation may be required to return soil quality should rapid salinization occur.

A state-of-the-art pilot treatment facility located onsite, which uses reverse osmosis and microfiltration to remove salt from the subsurface drainage entering the SJRIP facility, could play a role in the improved management of the salinity of the water applied to the alfalfa and tall wheatgrass crops within the SJRIP facility. However, the cost-effectiveness of this approach would need to be weighed against the profits generated from the forage sales. At present, the exorbitant cost of water treatment and the resulting high cost per m^3 of product water limits the further development of this

strategy. The major benefit currently realized by the SJRIP reuse facility is the disposal of drainage return flows and the associated salt load through crop evapotranspiration and direct evaporation. The successful optimization of the management deployed at the reuse facility will be essential for sustainable long-term operation and the facility's ability to serve the 43,000 ha Grasslands Drainage Area while meeting the zero drainage export requirements now in place. We suggest that this mandate be met with the newly designed rapid EM38-MK2-based soil salinity surveys, combined with a better suite of remote sensing tools to improve the automation of soil salinity mapping, combined with skilled technical support. Machine learning techniques may play a role in further streamlining this process. The Panoche Water District, in the meantime, is also expanding the SJRIP acreage (primarily with 'Jose' tall wheatgrass plantings) to meet the zero-drainage discharge mandate.

The goal of providing a user-friendly computer simulation model with an interactive graphical user interface (Figure 11) as a framework for the collection of relevant data for the development of water and salinity mass balances was fulfilled in this project. Given the dearth of data available at the beginning of the project and the difficulties interpreting the data that had been collected by the District, we were under no illusions that the model would be sufficiently calibrated to be used for prediction purposes. However, the CSUID-1D model was able to show its potential as a decision support tool to guide future management decisions and allow the SJRIP to achieve its drainage disposal function while providing an economic return through sustainable forage production. One significant oversight that was realized after the analysis of the 2016 data was the failure to include tile drains, drain depth and drainage yield among the CSUID-ID model input parameters that were selected at the beginning of the simulation. The original 3-D CSUID simulation code has significant capability for the depiction of tile drainage systems at the field and farm scale, but our initial thinking was to keep the model as simple as possible in order to keep run times short and not intimidate our targeted users. The EM38-MK2 results made clear the beneficial effect of tile drains in redistributing salts within the soil profile, with the highest concentration of salt in the lowest soil layer. Overall, the salt concentration was highest in the undrained fields. This oversight can be readily addressed in a new version of the CSUID-1D model user interface.

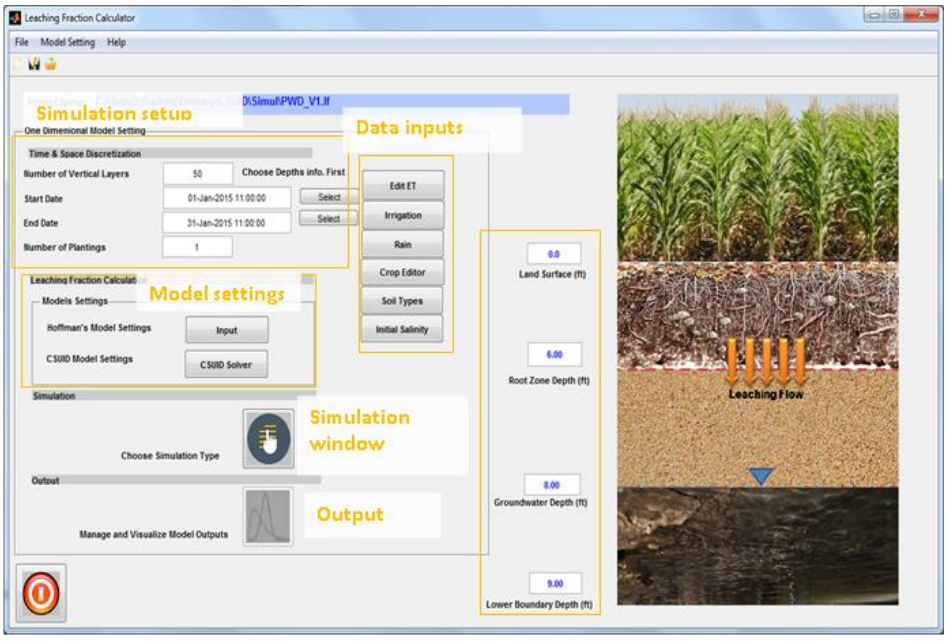

Figure 11. Graphical user interface for the CSUID-ID model that is being developed as a decision support tool for the estimation of the optimal leaching rates and the guidance of future irrigation blending decisions with lower EC water supply. The model has provided a useful framework for the assimilation of the required data for salinity mass balance assessments.

6. Future Work

The EM38-MK2 soil surveys were important for the characterization of the spatial variability of soil salinity in the fields included in this study and will have utility for the calibration and validation of the CSUID-1D computer model. Three years of field data is insufficient to obtain the credible calibration of the model. However, EM38 surveys require significant expertise to conduct, and time and effort and are unlikely to be continued by the District alone, given its resource limitations. Future collaborations with universities and project funding may allow the continuation of the EM38 mapping program. In the interim, the installation of representative cluster wells within each of the experimental fields may allow the District to track the salinity trends at two intervals within the soil profile using currently available resources and monitoring equipment. These wells will help assess the adequacy of current salt leaching practices, as well as providing data for the further calibration of computer-based model simulation tools that can serve as decision support systems. By developing a proxy relationship between each well and the average salinity at shallow (1.5–2.5 m) and deep (4.3–5.2 m) depths, the wells' EC data can be useful in showing trends in field salinization. Remote sensing using multispectral satellite imagery has shown some potential for salinity assessments when compared to field data; drone imagery avoids the problems associated with cloud cover, and it allows for image collection when conditions are closer to optimal. We are optimistic that higher resolution hyperspectral imagery may allow new spectral indices to be developed, which can assess the vegetation health and potential crop yield. These relationships could provide a more cost-effective means of tracking the soil salinity and preventing the onset of yield declines when the root zone salinity exceeds the yield response threshold. The regression models developed using soil salinity data and vegetation indices (NDVI, SAVI, RVI) yielded reasonable R-square values (exceeding 0.70). The best agreement was found to occur on the alfalfa field sites for the spring EM38-MK2 survey. We believe that we can achieve better results moving from satellite to drone-based imagery, in addition to increasing the palate of the spectral bands available to us by moving from multispectral to hyperspectral imagery.

The long-term aim is to have a credible, reliable and easy-to-use decision support tool that can guide future irrigation water quality management practices at the SJRIP, i.e., customizing the blend of subsurface drainage water and R.O. treatment plant product water to allow sustainable forage production in both alfalfa and 'Jose' tall wheatgrass fields.

Supplementary Materials: The following are available online at http://www.mdpi.com/2071-1050/12/16/6362/s1, Figure S1: Salinity distribution in the soil profile at the 12 sampling locations in tall wheatgrass field 13-16 for spring (left) and fall (right) surveys conducted in 2016 (upper) and 2017 (lower); Figure S2: Spatial distribution of average soil salinity for tall wheatgrass field 13-1 for the 0–120 cm depth (top two maps) and for each depth (bottom 8 maps) with (a) 0–30 cm, (b) 30–60 cm, (c) 60–90 cm and (d) 90–120 cm.; Figure S3: Salinity distribution in the soil profile at the 12 sampling locations in alfalfa field 13-2 for spring (left) and fall (right) surveys conducted in 2016 (upper) and 2017 (lower); Figure S4: Spatial distribution of average soil salinity for alfalfa field 13-2 for the 0–120 cm depth (top two maps) and for each depth (bottom 8 maps) with (a) 0–30 cm, (b) 30–60 cm, (c) 60–90 cm and (d) 90–120 cm.

Author Contributions: Conceptualization and funding acquisition for the research were performed by co-PI's S.E.B. and N.W.T.Q. S.E.B. and N.W.T.Q. were also responsible for project administration and the supervision of CSUF and LBNL staff who provided assistance on the project. Monitoring station design and the installation of the sensor network was performed by N.W.T.Q., together with the acquisition of irrigation application and field data from the Panoche Water District. S.E.B. was responsible for the agronomic and forage yield estimation. F.C. was responsible for the design of the EM surveys and soil sampling. The majority of the EM38 field surveys was performed by A.S. and various field staff assigned to this aspect of the work, including N.W.T.Q. and F.C. for the first field surveys. A.S. was responsible for the GIS mapping and laboratory salinity analysis, supervised and aided by S.E.B. This research is drawn largely from an M.S. thesis by A.S. that has been adapted with contributions from N.W.T.Q., S.E.B. and F.C. to conform with the guidelines for the Special Issue on Agricultural Sustainability and Policy. All authors have read and agreed to the published version of the manuscript.

Funding: Funding for the project was provided by the California Department of Water Resources under Grant Agreement No. 4600011273 with the Fresno State Foundation. Work for Others Agreement No. FP00003250 between Lawrence Berkeley National Laboratory Under Prime Contract No. DE-AC02-05CH11231 for the U. S. Department of Energy facilitated the Laboratory's involvement in the Project.

Acknowledgments: We are grateful for the support of the Panoche Drainage District staff; in particular, Manuel Cardoza and Juan Cadena, who provided assistance with instrument deployment, conducting EM38 soil surveys and collecting irrigation water samples. Ara Azhderian, Panoche Water District General Manager, has been consistently supportive of the project. Alan Penteriche, Lucas Ingold, Leandro Zambon, Ulysses Bottino Jr., Giuliano Galdi and Sangeeta Bansal assisted in collecting the field data, as well as the lab analysis. Tim Jacobsen, from the Center for Irrigation Technology (CIT), helped with the setup of the motorized survey equipment for the EM38 surveys.

Conflicts of Interest: The authors declare no conflict of interest. The funders had no role in the design of the study; in the collection, analyses, or interpretation of data; in the writing of the manuscript, or in the decision to publish the results.

Abbreviations

ALF, alfalfa; EC_a, apparent electrical conductivity; EC_e, electrical conductivity of the saturation soil paste extract; EC_{iw}, electrical conductivity of the irrigation water; EC_{sw}, electrical conductivity of the soil water; EMI, electromagnetic induction; ESAP, Environmental Sampling and Analysis Plan software; LF, leaching fraction; SJRIP, San Joaquin River Improvement Project; SJV, San Joaquin Valley; SJRB, San Joaquin River Basin; SJR, San Joaquin River; TMDL, Total Maximum Daily Load; TWG, tall wheatgrass.

References

1. Nachshon, U. Cropland soil salinization and associated hydrology: Trends, processes and examples. *Water* **2018**, *10*, 1030. [CrossRef]
2. Letey, J. Soil salinity poses challenges for sustainable agriculture and wildlife. *Calif. Agric.* **2000**, *54*, 43–48. [CrossRef]
3. Letey, J.; Williams, C.F.; Alemi, M. Salinity, drainage and selenium problems in the Western San Joaquin Valley of California. *Irrig. Drain. Syst.* **2002**, *16*, 253–259. [CrossRef]
4. Scudiero, E.; Corwin, D.L.; Anderson, R.G.; Yemoto, K.; Clary, W.; Wang, Z.; Skaggs, T.H. Remote sensing is a viable tool for mapping soil salinity in agricultural lands. *Calif. Agric.* **2017**, *71*, 231–238. [CrossRef]
5. Grattan, S.R.; Oster, J.D.; Letey, J.; Kaffka, S.R. Drainage Water Reuse: Concepts, Practices and Potential Crops. In *Salinity and Drainage in San Joaquin Valley, California: Science, Technology, and Policy*; Chang, A.C., Brawer Silva, D., Eds.; Springer: Dordrecht, The Netherlands, 2014; pp. 277–302. ISBN 978-94-007-6851-2.
6. Grattan, S.R.; Oster, J.D.; Benes, S.E.; Kaffka, S.R. Use of Saline Drainage Waters for Irrigation. In *Agricultural Salinity Assessment and Management*; American Society of Civil Engineers: Reston, VA, USA, 2011; Volume 22, pp. 687–719. ISBN 9780784476482.
7. Suyama, H.; Benes, S.E.; Robinson, P.H.; Getachew, G.; Grattan, S.R.; Grieve, C.M. Biomass yield and nutritional quality of forage species under long-term irrigation with saline-sodic drainage water: Field evaluation. *Anim. Feed Sci. Technol.* **2007**, *135*, 329–345. [CrossRef]
8. Suyama, H.; Benes, S.E.; Robinson, P.H.; Grattan, S.R.; Grieve, C.M.; Getachew, G. Forage yield and quality under irrigation with saline-sodic drainage water: Greenhouse evaluation. *Agric. Water Manag.* **2007**, *88*, 159–172. [CrossRef]
9. Cornacchione, M.V.; Suarez, D.L. Emergence, Forage Production, and Ion Relations of Alfalfa in Response to Saline Waters. *Crop Sci.* **2015**, *55*, 444–457. [CrossRef]
10. Benes, S.; Galdi, G.; Hutmacher, R.B.; Grattan, S.R.; Chahal, I.; Putnam, D.H. Opportunities for Management of Alfalfa (*Medicago sativa* L.) Under High Salinity Conditions. In Proceedings of the 2018 California Alfalfa and Forage Symposium, Reno, NV, USA, 27–28 November 2018.
11. Díaz, F.J.; Grattan, S.R.; Reyes, J.A.; de la Roza-Delgado, B.; Benes, S.E.; Jiménez, C.; Dorta, M.; Tejedor, M. Using saline soil and marginal quality water to produce alfalfa in arid climates. *Agric. Water Manag.* **2018**, *199*, 11–21. [CrossRef]
12. Schoups, G.; Hopmans, J.W.; Young, C.A.; Vrugt, J.A.; Wallender, W.W.; Tanji, K.K.; Panday, S. Sustainability of irrigated agriculture in the San Joaquin Valley, California. *Proc. Natl. Acad. Sci. USA* **2005**, *102*, 15352–15356. [CrossRef]
13. Oster, J.D.; Grattan, S.R. Drainage water reuse. *Irrig. Drain. Syst.* **2002**, *16*, 297–310. [CrossRef]
14. Suarez, D.L.; Wood, J.D.; Lesch, S.M. Effect of SAR on water infiltration under a sequential rain-irrigation management system. *Agric. Water Manag.* **2006**, *86*, 150–164. [CrossRef]

15. Quinn, N.W.T.; McGahan, J.C.; Delamore, M.L. Innovative strategies reduce selenium in Grasslands drainage. *Calif. Agric.* **1998**, *52*, 12–18. [CrossRef]
16. Linneman, C.; Falaschi, A.; Oster, J.D.; Kaffka, S.; Benes, S.E. Drainage Reuse by Grassland Area Farmers: The Road to Zero Discharge. In Proceedings of the Groundwater Issues and Water Management—Strategies Addressing the Challenges of Sustainability Meeeting, U.S. Committee on Irrigation and Drainage (US-CID), Sacramento, CA, USA, 4–7 March 2014.
17. Environmental Monitoring Systems Laboratory. *Methods for the Determination of Inorganic Substances in Environmental Samples (600/R-93/100)*; United States Environmental Protection Agency, Office of Research and Development: Cincinnati, OH, USA, 1993; Volume 600.
18. San Joaquin Valley Drainage Program. *A Management Plan for Agricultural Subsurface Drainage and Related Problems on the Westside San Joaquin Valley*; Final Report, September 1990; San Joaquin Valley Drainage Program: Sacramento, CA, USA, 1990.
19. Quinn, N.W.T. The San Joaquin Valley: Salinity and Drainage Problems and the Framework for a Response. In *Salinity and Drainage in San Joaquin Valley, California*; Chang, A.C., Brawer Silva, D., Eds.; Springer: Dordrecht, The Netherlands, 2014. [CrossRef]
20. Quinn, N.W.T. Policy Innovation and Governance for Irrigation Sustainability in the Arid, Saline San Joaquin River Basin. *Sustainability* **2020**, *12*, 4733. [CrossRef]
21. California Environmental Protection Agency. *Total Maximum Daily Load for Salinity and Boron in the Lower San Joaquin River*; Staff Report by the California Regional Water Quality Control Board, Central Valley Region, California Environmental Protection Agency: Sacramento, CA, USA, 2002.
22. Kratzer, C.R.; Pickett, P.J.; Rashmawi, E.A.; Cross, C.L.; Bergeron, K.D. *An Input Output Model of the San Joaquin River from the Lander Avenue Bridge to the Airport Way Bridge*; Appendix C of the California State Water Resources Control Board; Technical Committee Report on Regulation of Agricultural Drainage to the San Joaquin River; California State Water Resources Control Board: Sacramento, CA, USA, 1987; p. 173.
23. U.S. Bureau of Reclamation. *Grassland Bypass Project, Record of Decision and Final Environmental Impact Statement/Environmental Impact Report*; Entrix for Mid-Pacific Region, South-Central California Area Office: Fresno, CA, USA, 2009.
24. Brevik, E.C.; Fenton, T.E.; Lazari, A. Soil electrical conductivity as a function of soil water content and implications for soil mapping. *Precis. Agric.* **2006**, *7*, 393–404. [CrossRef]
25. Kelley, J.; Higgins, C.W.; Pahlow, M.; Noller, J. Mapping Soil Texture by Electromagnetic Induction: A Case for Regional Data Coordination. *Soil Sci. Soc. Am. J.* **2017**, *81*, 923–931. [CrossRef]
26. Weller, U.; Zipprich, M.; Sommer, M.; Castell, W.Z.; Wehrhan, M. Mapping Clay Content across Boundaries at the Landscape Scale with Electromagnetic Induction. *Soil Sci. Soc. Am. J.* **2007**, *71*, 1740. [CrossRef]
27. Corwin, D.L.; Lesch, S.M. Apparent soil electrical conductivity measurements in agriculture. *Comput. Electron. Agric.* **2005**, *46*, 11–43. [CrossRef]
28. Doolittle, J.A.; Brevik, E.C. The use of electromagnetic induction techniques in soils studies. *Geoderma* **2014**, *223*, 33–45. [CrossRef]
29. Corwin, D.L.; Lesch, S.M. Protocols and Guidelines for Field-scale Measurement of Soil Salinity Distribution with ECa-Directed Soil Sampling. *J. Environ. Eng. Geophys.* **2013**, *18*, 1–25. [CrossRef]
30. Corwin, D.L.; Lesch, S.M. Characterizing soil spatial variability with apparent soil electrical conductivity: I. Survey protocols. *Comput. Electron. Agric.* **2005**, *46*, 103–133. [CrossRef]
31. Lesch, S.M.; Rhoades, J.D.; Corwin, D.L. *The ESAP-95 Version 2.01R User Manual and Tutorial Guide. Research Report No. 146. USDA-ARS*; George, E.B., Jr., Ed.; Salinity Laboratory: Riverside, CA, USA, 2000.
32. Lesch, S.M.; Strauss, D.J.; Rhoades, J.D. Spatial Prediction of Soil Salinity Using Electromagnetic Induction Techniques: 2. An Efficient Spatial Sampling Algorithm Suitable for Multiple Linear Regression Model Identification and Estimation. *Water Resour. Res.* **1995**, *31*, 387–398. [CrossRef]
33. Rhoades, J.D. Soluble Salts. In *Methods of Soil Analysis: Part 2; Chemical and Microbiological Properties*; Page, A.L., Ed.; Monograph Number 9 (Second Edition); American Society of Agronomy: Madison, WI, USA, 1982; pp. 167–179.
34. Rhoades, J.D.; Manteghi, N.A.; Shouse, P.J.; Alves, W.J. Soil Electrical Conductivity and Soil Salinity: New Formulations and Calibrations. *Soil Sci. Soc. Am. J.* **1989**, *53*, 433–439. [CrossRef]
35. Letey, J.; Feng, G.L. Dynamic versus steady-state approaches to evaluate irrigation management of saline waters. *Agric. Water Manag.* **2007**, *91*, 1–10. [CrossRef]

36. Corwin, D.L.; Rhoades, J.D.; Šimůnek, J. Leaching requirement for soil salinity control: Steady-state versus transient models. *Agric. Water Manag.* **2007**, *90*, 165–180. [CrossRef]
37. Ben-Gal, A.; Ityel, E.; Dudley, L.; Cohen, S.; Yermiyahu, U.; Presnov, E.; Zigmond, L.; Shani, U. Effect of irrigation water salinity on transpiration and on leaching requirements: A case study for bell peppers. *Agric. Water Manag.* **2008**, *95*, 587–597. [CrossRef]
38. Lesch, S.M.; Strauss, D.J.; Rhoades, J.D. Spatial Prediction of Soil Salinity Using Electromagnetic Induction Techniques: 1. Statistical Prediction Models: A Comparison of Multiple Linear Regression and Cokriging. *Water Resour. Res.* **1995**, *31*, 373–386. [CrossRef]